Title
Cyclic heating effects on thermal volume change of silt

Journal
Environmental Geotechnics, 2(5)

ISSN
2051-803X

Authors
Vega, Alexander
McCartney, John S

Publication Date
2015-10-01

DOI
10.1680/envgeo.13.00022

Peer reviewed

- Article type: Technical paper
- Date text written: August 16, 2013
- 5334 words and 10 illustrations.

Cyclic Heating Effects on Thermal Volume Change of Silt

Alexander Vega, M.S.

- Engineer
- Brierley and Associates, Denver, Colorado USA

John S. McCartney, Ph.D., P.E.

- Associate Professor and Lyall Faculty Fellow
- Department of Civil, Environmental and Architectural Engineering, University of Colorado Boulder, UCB 428, Boulder, USA

Contact details of corresponding author:

John S. McCartney, Ph.D., P.E.
Associate Professor and Lyall Faculty Fellow
University of Colorado Boulder
Department of Civil, Environmental and Architectural Engineering
UCB 428
Boulder, CO 80309
john.mccartney@colorado.edu
Phone: +001-303-492-0470

Abstract (200 words)

This study focuses on the thermal volume change of compacted, saturated silt during temperature cycles. A temperature-regulated oedometer with backpressure control was used to measure the thermal consolidation of silt specimens under normally consolidated to heavily overconsolidated initial stress states. During initial heating, the silt specimens displayed thermal volume changes similar to those reported in the technical literature, with the normally consolidated specimen showing contraction and heavily-overconsolidated specimens showing expansion. The specimens all showed elastic contraction during cooling, as expected. However, subsequent heating and cooling cycles led to additional permanent volume change. This observation contradicts thermo-elasto-plastic theories which predict plastic contraction only during initial heating of soils with low overconsolidation ratios, and predict elastic volume changes during subsequent heating and cooling cycles. A source of error in the experiments was a softer response during heating due to differential radial expansion of the oedometer ring, followed by exaggerated axial expansion of the soil during cooling when the ring contracted. Nonetheless, the accumulation of permanent strain during cyclic heating and cooling indicates that the thermal yield surface history may not be locked in during the cooling process, implying that kinematic thermal hardening or thermal creep mechanisms should be explored.

Keywords chosen from ICE Publishing list
Geotechnical Engineering, Piles and Piling, Renewable Energy.

List of notation (examples below)

α	is the coefficient of linear thermal expansion
ΔT	is the change in temperature measured at the top of the oedometer specimen
e	is the void ratio
ε^{T}	is the thermal axial strain
σ'_a	is the axial effective stress
ΔH	is the change height of the oedometer specimen
Δu	is the change in pore water pressure

1. Introduction

Ground-source heat pumps (GSHPs) are a well-established technology used to provide energy efficient heating and cooling to buildings by exchanging heat with the subsurface soil or rock, which has a relatively constant temperature compared to that of the outside air (Omer 2008). Although heating and cooling may lead to thermally-induced volume change of the ground surrounding a heat exchanger installed in a borehole or trench, this behaviour is typically ignored in the analysis and design of GSHP systems. This is not the case when heat exchangers are embedded within the foundations of buildings to form "energy foundations". Energy foundations and other types of thermally active geotechnical systems not only serve their conventional purpose (e.g., providing structural support, grade separation, earth retention, etc.) but also provide a pathway for heat exchange with the subsurface for little additional construction cost (Laloui et al. 2003; Brandl 2006; Adam and Markiewicz 2009). Temperature fluctuations within an energy foundation during heat exchange operations may lead to permanent thermal volume changes in the surrounding soil that may affect the performance of the energy foundation or the overlying superstructure. An understanding of the mechanisms of thermal volume change of soils under different stress states and temperature cycles may help improve the interpretation of axial strain measurements from energy foundations during heating and cooling operations (Laloui et al. 2006; Amatya et al. 2012; McCartney and Murphy 2012). A schematic of a soil element next to an energy foundation is shown in Figure 1, highlighting the relative magnitudes of thermal volume change in the horizontal and vertical directions expected from measurements of thermal volume changes of soils under anisotropic stress states (Coccia and McCartney 2012). Potential effects of thermal volume changes on energy foundations are also noted in Figure 1, including dragdown and changes in lateral confinement of the foundation.

The impact of temperature cycles on soil volume change has not been fully investigated. Energy foundations experience relatively slow fluctuations in temperature over time due to heating and cooling demands from the building, with temperatures potentially ranging from 3 to 35 °C (McCartney and Murphy 2012). Campanella and Mitchell (1968) observed an isotropic permanent contraction of a saturated specimen of normally consolidated Illite clay during initial heating, followed by elastic contraction during cooling. Although this behaviour has since been observed in several other studies because of mechanisms that will be discussed in the next section, Campanella and Mitchell (1968) also observed a comparatively small amount of additional contraction during successive cycles. They attributed this to cyclic stabilization and the effects of thermal creep. Continued isotropic volume changes of high plasticity clays during cyclic heating and cooling were also observed by Burghignoli et al. (1992), confirming that this phenomenon occurs for other soil types. Despite these observations, the amount of additional thermal volume change expected after cyclic heating and cooling is not well understood for soils with different initial stress states. This information would be useful for evaluating the long-term performance of energy foundations in different soil deposits. Further, these continued volume changes during temperature cycles cannot be explained using current thermo-elasto-plastic constitutive models for volume change (Hueckel and Borsetto 1990; Cui et al. 2000; Laloui and Cekeravac 2003; Abuel-Naga et al. 2007a). Accordingly, the objective of this study is to confirm the impact of cyclic heating and cooling on the thermal volume change of saturated silt specimens under different initial stress states in order to guide the refinement of thermal hardening mechanisms in these constitutive models.

2. Background

Early nonisothermal studies of soil volume change focused on the effects of temperature changes between 30 and 50 °C on soil samples during sampling, storage, and transportation (Gray 1936; Finn 1951; Paaswell 1967; Campanella and Mitchell 1968; Plum and Esrig 1969). Later studies evaluated the behaviour of soils under temperatures greater than 60 °C for applications such as buried high-voltage electric cables (Abdel-Hadi and Mitchell 1981), heated oil and gas pipelines (Slegel and Davis 1977), and the disposal of nuclear waste in offshore soft clay deposits (McGinley 1983; Houston et al. 1985) or clay-encapsulated repositories (Baldi et al. 1988). Several fundamental studies have been performed on different saturated fine-grained soils to investigate their response to the combined effects of stress state and temperature (Demars and Charles 1982; Hueckel and Baldi 1990; Towhata et al. 1993; Burghignoli et al. 1992, 2000; Sultan et al. 2002; Romero et al. 2003; Cekerevac and Laloui 2004; Abuel-Naga et al. 2007b). Other fundamental studies have evaluated the role of unsaturated conditions (Saix et al. 2000; Uchaipichat and Khalili 2009; Tang and Cui 2009). Recent interest in thermally active geotechnical systems, including energy foundations, has continued to drive the interest in the temperature effects on soils. These systems differ from those studied in the past as they undergo cycles of heating and cooling over time (Brandl 2006).

Different from other engineering materials like steel or concrete, heating of a soil element in drained conditions to temperatures in the ranges mentioned above may lead to both recoverable (elastic) and permanent (plastic) volume changes. Campanella and Mitchell (1968) and Paaswell (1967) proposed several mechanisms of volume change in water-saturated soils. In the absence of clay minerals, which may be affected by temperature changes, the elastic and plastic volume changes arise primarily due to the elastic differential expansion and contraction of the soil skeleton and pore water. Specifically, the coefficient of thermal expansion of pore water is approximately 7-10 times that of most soil particles (McKinstry 1965; Mitchell and Soga 2005). In drained heating tests on normally consolidated and lightly overconsolidated soils, the differential expansions of water and soil particles lead to excess pore water pressure generation (Houston et al. 1985; Abuel-Naga et al. 2007b), which dissipates resulting in a time-dependent, irrecoverable volumetric contraction of the soil (Sultan et al. 2002; Vega et al. 2012). In undrained heating tests excess pore water pressures are generated, although no permanent volume change will occur as drainage and consolidation are not permitted. Plum and Esrig (1969) performed a cyclic heating test on an undrained specimen of low plasticity clay, and observed an increase in excess pore water pressure with each cycle until stabilizing after four heating-cooling cycles. Their observation supports the mechanism of thermal volume change in normally consolidated soils and the cyclic effects observed by Campanella and Mitchell (1968). Additionally, normally consolidated soils having a greater plasticity index (i.e., more active clay minerals) show greater plastic volume change during heating (Sultan et al. 2002). Other mechanisms of thermal volume change that have been proposed include the effects of a decrease in water viscosity with temperature and thermal creep associated with changes in individual particle contact stresses with increased temperature.

Thermal volume changes are also dependent on the stress state. Saturated soils with overconsolidation ratios (OCRs) greater than 1.5 to 3 tend to expand elastically during heating (Paaswell 1967; Plum and Esrig 1969; Demars and Charles 1982; Baldi et al. 1988; Hueckel and Baldi 1990; Towhata et al. 1993; Delage et al. 2000; Cekeravac and Laloui 2004). The physical reason that overconsolidated clays expand upon heating has not been explained in a similar manner to the mechanisms of thermal volume change of normally consolidated soils. It is possible that the soil skeleton of overconsolidated clays is stiffer, making them tend to behave more like a continuous, single-phase, thermo-elastic material during heating and cooling. However, some studies have observed that heating of overconsolidated clays above a certain temperature may cause plastic contraction (Baldi et al. 1988; Towhata et al. 1993; Cui et al. 2000; Cekeravac and Laloui 2004). Coccia and McCartney (2012) observed that anisotropic stress states may lead to thermal expansion and contraction in the same soil specimen in different directions. They tested a specimen of saturated Bonny silt that was initially loaded isotropically in a temperature-controlled cubical cell, unloaded in one direction, then heated uniformly. Expansion was observed during heating in the direction of lower stress (greater overconsolidation ratio), while contraction was observed during heating in the direction of greater stress (lower overconsolidation ratio). Unsaturated conditions also affect the thermal volume change of soils. Uchaipichat and Khalili (2009) observed that unsaturated compacted silt specimens expand during heating under low net normal stress values (high overconsolidation ratios) and contract during heating under higher net normal stress values (lower overconsolidation ratios).

Interest in clay barriers for nuclear waste disposal and thermally active geotechnical systems prompted the development of thermo-elasto-plastic constitutive relationships to predict thermal volume changes of soils noted in the experimental studies mentioned above (Hueckel and Borsetto 1990; Cui et al. 2000; Cekeravac and Laloui 2004; Abuel-Naga et al. 2007b). The models are generally based on the Modified Cam Clay model, and indicate that plastic, contractive thermal volume changes should only occur on the first heating cycle of normally consolidated soil, or possibly when heating an overconsolidated soil above a certain temperature if an additional hardening mechanism is incorporated (Cui et al. 2000). In either case, this initial heating process leads to an expansion of the yield surface. This means that subsequent cooling and heating cycles below the previously applied temperature should lead only to elastic, expansive thermal volume changes. Accordingly, most existing constitutive models do not have the capability to capture the cyclic effects observed by Campanella and Mitchell (1968) and Burghignoli et al. (1992). Although small, the continued displacements they observed during cyclic heating and cooling may have a long-term impact on thermally active geotechnical systems. Advanced constitutive models such as that described by Hueckel and Pellegrini (1996) have incorporated rotational kinematic yield surfaces to account for anisotropic strains measured in compacted specimens, which may provide a strategy for accounting for these cyclic effects. Additional information on the role of cyclic heating and cooling tests for different stress states than those investigated by Campanella and Mitchell (1968) and Burghignoli et al. (1992) is still required to provide calibration data for these advanced constitutive models.

3. Materials and Methods

3.1 Materials

Soil from the Bonny dam located near the Colorado-Kansas, referred to as “Bonny silt”, was used in this experimental study. The thermal volume change of this soil has been characterized in previous experimental studies (El Tawati 2010; Coccia and McCartney 2012; Vega et al. 2012), and it has been used extensively in centrifuge experiments on energy foundations including those with cycles of heating and cooling (McCartney and Rosenberg 2011; Stewart 2012). The particle-size distribution of Bonny silt is shown in Figure 2(a), along with different characteristic particle sizes. Because of the high fines content, the silt is expected to behave as a low-permeability material that can retain stress history. Bonny silt has a plasticity index of 4, so it can be classified as ML according to the Unified Soil Classification Scheme (USCS). The silt has a relatively low activity of 0.29, which indicates that the fines do not contain a significant amount of clay minerals that may be affected by temperature (Mitchell and Soga 2005). The thickness of the diffuse double layer of some clay minerals is sensitive to temperature, so high amounts of clay minerals such as Smectite may lead to complex thermo-hydro-mechanical behaviour (Sultan et al. 2002). The specific gravity of Bonny silt is 2.63.

Compaction curves were obtained for Bonny silt using the standard and modified Proctor compaction tests, and are presented in Figure 2(b). The specimens evaluated in this study were prepared using static compaction with a manual press in order to lead to similar soil conditions to those used in centrifuge tests on energy foundations by McCartney and Rosenberg (2011) and Stewart (2012). The target compaction conditions for the clay specimens were a compaction water content of 15% and a dry unit weight γ_{dry} of 16.3 kN/m^3, which correspond to 1.4% wet of optimum at the maximum dry density according to the standard Proctor compaction curve. The soil specimen was compacted in two lifts of equal thickness under a static load of 300 kPa. The interface between the lifts was scarified to minimize the likelihood of a weak zone within the specimen.

The thermal conductivity for a Bonny silt specimen under these compaction conditions was measured using the methodology described by McCartney et al. (2013). The thermal conductivity as a function of void ratio was measured for a specimen saturated using backpressure in a triaxial cell modified to accommodate a thermal needle probe inserted into the soil specimen through the top platen. The results shown in Figure 2(c) indicate that the thermal conductivity ranges from 1.37 to 1.47 W/(mK) for the range of void ratios evaluated in this study. The hydraulic conductivity of the Bonny silt in saturated conditions was measured in a flexible wall permeameter, and is 6×10^{-8} m/s for a void ratio of 0.55.

3.2 Thermal Oedometer

A temperature-regulated oedometer developed by McGinley (1983) and modified by El Tawati (2010) was used in this study to evaluate the thermo-mechanical response of compacted silt during heating and cooling cycles. An innovative aspect of this oedometer compared to other thermal oedometers is that it is contained within a pressure cell that can be used to saturate the soil specimen using backpressure before consolidation testing. A cross-section schematic of the pressure cell is shown in Figure 3(a), and a picture of the thermal oedometer, external mechanical loading system and heating system is shown in Figure 3(b). All of the main components of the pressure cell were made of stainless steel (TYPE 316) to resist corrosion, withstand high pressures, and permit high temperature ranges. Use of the same material for all of the components is expected to lead to minimal differential expansion and contraction during temperature changes. The pressure cell is a cylinder having a diameter of 153 mm and a height of 127 mm, sealed with “O”-rings between two 25.4-mm thick end caps. This assembly is held together with three 12.7-mm diameter steel rods on the outside of the cylinder. Electrical resistance-type tubular heating coils are integrated into the cylinder of the pressure cell and are used to heat the cell water during testing. The end caps of the pressure cell include several ports for control of the water pressure within the cell, circulation of water to homogenize temperatures, and instrumentation access, as shown in Figure 3(a). A loading piston sealed to the top of the cell with a rolling diaphragm is used to apply mechanical loads and measure displacements on the specimen. A pneumatic air cylinder was used to generate the static axial load applied to the specimen, and axial loads were monitored using a Brainard-Kilman E-210, S-type load cell. Axial movement of the specimen were monitored using a linear variable deformation transformer (LVDT), with the core of the LVDT mounted on the loading piston outside of the pressure cell.

The soil specimen is confined within a cylindrical consolidation ring having an inner diameter of 83 mm, a height of 25.4 mm, and a wall thickness of 3.2 mm. The consolidation ring and the specimen can be removed from the system for initial compaction of the soil specimen within the ring. To help reducing friction between the consolidation ring and the travelling loading piston, the inner surface of the ring is coated with Teflon paint. The oedometer is configured to have free drainage at the upper boundary of the specimen and no drainage at the bottom of the specimen. This configuration allows for pore water pressure measurement at the bottom boundary of the specimen. Thermal radial expansion of the consolidation ring will not result in purely oedometric (zero lateral strain) conditions, which may have an impact on the thermal volume changes of the soil (Burghignoli et al. 1995; Abuel-Naga et al. 2007b).

The pressure applied to the cell fluid (de-aired water) is controlled using the backpressure reservoir shown in Figure 3(b). The valve connecting the backpressure reservoir and the pressure cell was maintained open throughout testing, which permitted free drainage of water from the soil specimen during mechanical or thermal consolidation. The pore water pressure at the base of the specimen was monitored using a differential pressure transducer (DPT) manufactured by Validyne Engineering (model P305D). The DPT is used to measure the difference in water pressure between the lower and upper boundaries of the specimen. It is assumed that the water pressure at the top of the specimen should remain constant during the test, so changes in the DPT reading are assumed to be representative of the changes in pore water pressure at the base of the soil specimen in the single-sided drainage oedometer.

A Watlow temperature regulator was used to control the temperature of the heating coil surrounding the soil specimen. A tip-sensitive stainless steel sheathed Type J thermocouple probe (labelled as Thermocouple 1 in Figure 3(a)) was used to measure the temperature of soil specimen. Thermocouple number 1 extends through the loading piston to the top side of the upper porous disk, and is assumed to provide a reasonable estimate of the temperature at the top surface of the center of the specimen. Changes in temperature measured using a second thermocouple probe in the cell fluid (labelled as Thermocouple 2 in Figure 3(a)) provide feedback to the temperature regulator. To enhance uniformity of temperature in the pressure cell, a circulation pump having an operating range up to 100°C (model PQM-1 from Greylor Company) was used to homogenize the pressurized cell fluid.

3.3 Characterization of Machine Deflections

It is critical to evaluate the machine deflection of the thermal oedometer during both mechanical loading and subsequent temperature changes. The machine deflections were evaluated by placing a disk of tool steel (E = 210 GPa, $\alpha = -13 \times 10^{-6}$ m/m°C) having a height of 25.4 mm and a diameter of 75 mm (slightly smaller than that of the inside of the consolidation ring to avoid potential Poisson effects or differential lateral expansion during heating) within the oedometer. The mechanical machine deflections were defined by subtracting the known thermal displacements of the steel disk from the measured LVDT readings. The oedometer system was observed to deform linearly during loading and unloading, as shown in Figure 4. Thermal machine deflections were characterized while the steel disk was under the maximum axial stress applied in the testing program, following a heating and cooling cycle similar to that applied to the soil specimens. Time series from this machine deflection test are shown in Figure 5(a). The thermal machine deflections calculated by subtracting the thermo-elastic response of the steel disk from the measured displacements are shown as a function of temperature in Figure 5(b). The thermal machine deflection was observed to follow a nonlinear trend during heating, while it followed a nearly linear trend during cooling. Repeated tests indicate that regardless of the maximum temperature applied to the oedometer cell, the same cooling slope was noted, with the system returning to a height smaller than initially measured. This is attributed to the interaction between the different components of the pressure cell, especially the vertical rods holding the pressure cell together (which are not heated) and the "O"-ring seals. Although a second heating cycle was not performed for this particular test, other preliminary calibration tests indicate that the thermal machine deflection on the second cycle starts from the positive displacement of 0.04 mm and follows a hyperbolic trend that merges with the original heating test after a temperature change of approximately 40 °C.

Abuel-Naga et al. (2007b) assumed constant volume conditions to estimate the axial strain of a soil specimen due to radial thermal expansion of the oedometer ring during heating, and concluded that this axial strain was a relatively small compared to the thermal axial strain of the soil. However, one of the issues involved in cyclic testing is the radial contraction of the ring against the soil specimen during cooling. Thermal contraction of the soil may lead to increased contact between the ring and the soil, so the radial contraction of the ring during cooling may have greater effects on the measured volume change of the soil than the radial expansion of the ring during heating. Further, the radial expansion and contraction of the oedometer ring may occur at different times than the thermal volume change of the soil due to the particular thermal boundary conditions in this oedometer. These effects can be observed through evaluation of the thermal volume changes of the soil. The coefficient of thermal expansion of steel is not very different from that of most overconsolidated soils (10 to 13 × 10^{-6} m/m°C), so the effects of the thermal expansion of the oedometer ring are only expected to play an important role in the transient heating response of the specimen. Conclusions drawn from the values at equilibrium under a given temperature are expected to provide an accurate representation of the soil behaviour.

3.4 Experimental Approach

After static compaction of a soil specimen within the oedometer ring using a mechanical press, this assembly was placed into the thermal oedometer and the pressure cell was assembled. A vacuum of -85 kPa was applied to the cell to initially de-air the specimen and cell. Application of the vacuum to the cell led to application of a seating load to the specimen as the axial piston was free to move during this process. De-aired water was then permitted to slowly infiltrate upward through the specimen while maintaining vacuum on the pressure cell. After at least 3 pore volumes had infiltrated through the specimen, the cell and all plumbing lines (including the circulation pump) were filled with de-aired water. The axial stress (controlled using the pneumatic air cylinder) and backpressure were increased in stages to maintain the initial seating load on the specimen until reaching a backpressure of 210 kPa. Time was permitted for dissolution of any remaining air bubbles in the soil specimen. Next, the compacted silt specimen was mechanically consolidated in an incremental manner until reaching a stress representative of normally consolidated conditions, as shown in Figure 6.

The thermal consolidation behaviour of five specimens were evaluated in this study, each having a different initial stress state. After loading a given specimen to normally consolidated conditions, they were unloaded by different amounts to reach overconsolidation ratio (OCR) values of 1.00, 1.28, 1.80, 7.36, and 30.29. The compression curves for the five specimens are shown in Figure 7, along with the compression index and the average recompression index. The specimen conditions after compaction along with the conditions at the end of mechanical loading are summarized in Table 1. Two of the specimens were loaded to slightly higher values before being unloaded, but it is assumed that the stress state has a greater impact on thermal volume change than the initial void ratio. The role of the initial void ratio on the thermal volume change has not been evaluated thoroughly, and deserves further study through investigation of specimens with the same OCR but different void ratios. In this study, the three lower OCR values are expected to represent normally consolidated to lightly overconsolidated behaviour, while the two higher OCR values are expected to represent heavily overconsolidated behaviour. Next, each specimen was subjected to a four cycles of heating and cooling up to a maximum temperature change of 75 °C, as shown in Figure 6. Although this temperature is greater than that experienced by thermally active geotechnical systems, it represents a worst-case scenario. Heating was applied during each cycle at the fastest rate permitted by the temperature regulator (approximately 1.54 °C/hr), followed by unassisted cooling back to ambient room temperature. Each subsequent temperature cycle was conducted by applying the same rates of fast heating to the silt followed by unassisted cooling to room temperature. After each individual thermal consolidation test, the specimens were unloaded, removed from the temperature regulated oedometer, and oven-dried to measure the final water content.

4. Results

The axial stress and temperature applied to the normally consolidated specimen (OCR 1.00) during the first heating-cooling cycle are shown in Figure 8(a). The axial stress was approximately constant during testing. The measured change in height, the machine deflection obtained from Figure 5(b), and the corrected change in height of the soil are shown in Figure 8(b). The measured change in height is less than the machine deflection, which implies that the specimen is contracting. During cooling, the specimen is observed to expand slightly, which is attributed to the radial contraction of the oedometer ring. The pore water pressure measured using the DPT is also shown in Figure 8(b). Although the specimen was heated in drained conditions, a pore water pressure of 9.3 kPa (0.7% of the axial stress) was measured. Although the temperature change peaked after 1200 s, the pore water pressure peaked after 500 s. This implies that drainage was occurring simultaneously with the heating process. The rate of deformation started to slow after the pore water pressure peaked. The temperatures and axial stress during all four heating-cooling cycles for the normally consolidated specimen are shown in Figure 8(c), while the pore water pressure and displacement during all of the cycles are shown in Figure 8(d). The only interesting observation during the repeated cycles is that the pore water pressure generated on the 3rd, 4th, and 5th cycles decreased with each cycle, but they were all slightly greater than during the first cycle. Despite these greater pore water pressures, the amount of thermal contraction upon heating decreased with each cycle. Pore water pressures of the magnitude observed in Figure 8(d) were only noted for the normally consolidated specimen. A maximum change in pore water pressure of 2 kPa was observed for the specimens having greater OCR values, and a transitional behaviour was not noted in the pore water pressure response for lightly overconsolidated soils.

The thermal axial strain as a function of temperature for the normally consolidated specimen is shown in Figure 9(a). The specimen was observed to contract nonlinearly with increasing temperature. The effect of radial expansion of the ring was not clearly observed on the initial contraction of the specimen, although it likely led to a softer response. However, during cooling, the effect of the radial contraction of the ring is more significant. The thermal machine deflections do not incorporate this effect because the steel disk used in the calibration test had a slightly smaller diameter than that of the inside of the oedometer ring. The radial contraction of the ring likely occurred primarily at the beginning of the cooling process as it cooled faster than the soil inside the ring, leading to a greater amount of soil expansion. After reaching a temperature change of about 60°C, the soil contracted elastically during cooling, leaving a permanent axial strain of 0.48%. The next heating cycle was observed to lead to a relatively elastic response similar to the cooling curve until a temperature change of about 40 °C, after which the soil started to contract again. The effect of the ring contraction was observed again upon cooling, but the shape of the second cooling curve was relatively consistent with that of the cooling curve from the first cycle. An additional plastic axial contraction of 0.14% was observed during the second heating-cooling cycle. Similar behaviour was noted on the next two heating-cooling cycles, with the amount of thermal contraction decreasing slightly with further cycles.

The thermal volume change results from the tests on specimens with OCR values of 1.28, 1.80, 7.36, and 30.29 are shown in Figures 9(b), 9(c), 9(d), and 9(e), respectively. Comparing the thermal volume changes for the specimens with different OCR values, the trends are similar to those observed in the literature, with a transition from contractive to expansive behaviour with increasing OCR (Baldi et al. 1988; Cekeravac and Laloui 2004; Abuel-Naga et al. 2007b). Further, regardless of the OCR value, the values of α were relatively consistent and reflected elastic contraction. Specifically, the values of α obtained from the slopes of the cooling curves ranged from -5 to -13 × 10^{-6} m/m°C, which is a reasonable range for silt. The impact of the radial contraction of the consolidation ring during cooling was observed to increase with increasing OCR, possibly because of the expansion of the soil radially during the heating process that led to greater radial stresses than in the normally consolidated case. This behaviour led to a slight hysteresis loop in the thermal volume change curves. Nonetheless, similar to the normally consolidated soil, the overconsolidated soils also experienced additional plastic thermal volume change during each cycle. However, the magnitude of additional plastic thermal volume change decreases with increasing OCR.

5. Analysis

A summary of the permanent thermal axial strains at the end of a heating-cooling cycle for each of the silt specimens having different OCR values is shown in Figure 10(a). A slight increasing trend is noted for the three specimens with low OCR values, with a greater initial thermal axial strain value. A relatively flat trend is noted for the heavily overconsolidated specimens. The permanent thermal axial strain as a function of OCR for each of the heating-cooling cycles is shown in Figure 10(b), which clearly reveals an upward shift in the curves at low OCRs with increasing numbers of heating-cooling cycles. The results are also plotted in terms of the permanent thermal axial strain divided by the change in temperature in Figure 10(c). The range of magnitude of the data in this figure, along with the trend with OCR, are consistent with those for similar soils reported in the literature (McCartney 2012). The results in Figure 10 indicate that a rotational kinematic hardening mechanism such as that described by Hueckel and Pellegrini (1996) may be suitable to capture the cyclic thermal volume changes noted in this study as well as those by Campanella and Mitchell (1996) and Burghignoli et al. (1992). Alternatively, a thermal creep factor may be used to account for additional permanent volume changes during subsequent heating cycles for normally consolidated soils.

The observations in Figure 10 have positive implications on the implementation of energy foundations, which are often installed in overconsolidated soil layers through which it may be difficult to drive piles. If the soil is initially normally consolidated, the results from thermal oedometer tests performed with a single heating-cooling cycle may need to be modified to account for more than a 50% increase in thermal volume changes during subsequent cycles. The magnitude of thermal volume change observed for normally consolidated specimens indicates that dragdown will likely occur for energy foundations intersecting normally consolidated soil deposits, as the displacements required to mobilize side shear stresses in deep foundations are relatively small. As most of the energy foundations reported in the literature have been installed in relatively overconsolidated soil deposits (Laloui et al. 2006; Amatya et al. 2012; McCartney and Murphy 2012), further research is needed to confirm if this behaviour is noted in energy foundations in normally consolidated soil deposits.

6. Conclusions

A series of five thermal consolidation tests were performed on saturated silt specimens having different initial stress states with a thermal oedometer having single-drainage boundary conditions. In each test, four cycles of heating and cooling with a temperature change of 75 °C were applied, during which changes in axial deformation and pore water pressure were measured. The following conclusions can be drawn from this study:

- During the first heating phase, the normally consolidated silt specimens were observed to show permanent contraction while the overconsolidated silt specimens were observed to show expansion. During the subsequent cooling phase, all specimens were observed to show elastic contraction.
- During additional heating and cooling phases, the specimens all showed a small amount of additional contraction, regardless of the stress state. The normally consolidated specimen showed the greatest amount of additional permanent contraction.
- Changes in pore water pressure were noted during each heating cycle for the normally consolidated specimen, supporting the axial deformation results that indicate that continued permanent contraction occurs during each heating and cooling cycle. Specimens with a greater overconsolidation ratio show less pore water pressure generation during heating.
- The machine deformations were observed to plan an important role in the final thermal volume change results. The effect of the radial contraction of the oedometer ring during cooling was found to be a function of the overconsolidation ratio of the soil.

Acknowledgements

Financial support from NSF grant CMMI 0928324 is gratefully acknowledged. The contents of this paper reflect the views of the authors and do not necessarily reflect the views of the sponsor.

References

Abdel-Hadi, ON and Mitchell, JK (1981) Coupled heat and water flows around buried cables. Journal of the Geotechnical Engineering Division 107(11): 1461–1487.

Abuel-Naga HM, Bergado DT, Bouazza A, and Ramana GV (2007a) Volume change behavior of saturated clays under drained heating conditions: Experimental results and constitutive modeling. Canadian Geotechnical Journal 44: 942-956.

Abuel-Naga HM, Bergado DT, and Bouazza A (2007b) Thermally induced volume change and excess pore water pressure of soft Bangkok clay. Engineering Geology 89: 144-154.

Adam D and Markiewicz R (2009) Energy from earth-coupled structures, foundations, tunnels and sewers. Géotechnique 59(3): 229–236.

Amatya BL, Soga K, Bourne-Webb PJ, Amis T, and Laloui L (2012) Thermo-mechanical behaviour of energy piles. Géotechnique 62(6): 503–519.

Baldi G, Hueckel T, and Pellegrini R (1988) Thermal volume changes of the mineral-water system in low-porosity clay soils. Canadian Geotechnical Journal 25: 807–825.

Brandl H (2006) Energy foundations and other thermo-active ground structures. Géotechnique. 56(2): 81-122.

Burghignoli A, Desideri A, and Miliziano S (1992) Deformability of clays under non-isothermal conditions. Revista Italiana di Geotechnica. 4/92: 227-236.

Burghignoli A, Desideri A, Miliziano S (1995) Discussion of volume change of clays induced by heating as observed in consolidation test. Soils and Foundations 35(1): 122-124.

Burghignoli A, Desideri A, and Miliziano S (2000) A laboratory study on the thermomechanical behaviour of clayey soils. Canadian Geotechnical Journal. 37: 764-780.

Campanella RG and Mitchell JK (1968) Influence of temperature variations on soil behavior. Journal of the Soil Mechanics and Foundation Engineering Division 94(SM3): 709–734.

Cekeravac C and Laloui L (2004) Experimental study of thermal effects on the mechanical behavior of a clay. International Journal for Numerical Analytical Methods Geomechanics, 28: 209–228.

Coccia CJR and McCartney JS (2012) A thermo-hydro-mechanical true triaxial cell for evaluation of the impact of anisotropy on thermally-induced volume changes in soils. ASTM Geotechnical Testing Journal 35(2): 11 pg.

Cui Y-J, Sultan N, and Delage P (2000) A thermomechanical model for clays. Canadian Geotechnical Journal 37(3): 607–620.

Delage P, Sultan N, and Cui YJ (2000) On the thermal consolidation of Boom clay. Canadian Geotechnical Journal 37(2): 343–354.

Demars KR and Charles RD (1982). Soil volume changes induced by temperature cycling. Canadian Geotechnical Journal 19: 188–194.

El Tawati A (2010) Impact of the Rate of Heating on the Thermal Consolidation of Compacted Silt. M.S. Thesis. University of Colorado Boulder.

Finn FN (1951) The effects of temperature on the consolidation characteristics of remolded clay. Symposium on Consolidation Testing of Soils, ASTM, Special Technical Publication, No. 126: 65–72.

Gray H (1936) Progress report on the consolidation of fine-grained soils. In Proc. of the 1st Int. Conf. on Soil Mechanics and Foundation Engineering, Cambridge, Mass., 138–141.

Houston SL, Houston WN, and Williams ND (1985) Thermo-mechanical behavior of seafloor sediments. Journal of Geotechnical Engineering. 111(12): 1249-1263.

Hueckel T and Baldi M (1990) Thermoplasticity of saturated clays: experimental constitutive study. Journal of Geotechnical Engineering 116(12): 1778–1796.

Hueckel T and Borsetto M (1990) Thermoplasticity of saturated soils and shales: Constitutive equations. Journal of Geotechnical Engineering 116(12): 1765-1777.

Hueckel T and Pellegrini R (1996) A note on thermomechanical anisotropy of clays. Engineering Geology 41: 171-180.

Laloui L and Cekeravac C (2003) Thermo-plasticity of clays: An isotropic yield mechanism. Computers and Geotechnics 30: 649-660.

Laloui L. Moreni M, and Vulliet L (2003) Comportement d'un pieu bi-fonction, foundation et échangeur de chaleur. Canadian Geotechnical Journal 40(2): 388-402.

Laloui L, Nuth M, and Vulliet L (2006) Experimental and numerical investigations of the behaviour of a heat exchanger pile. International Journal of Numerical and Analytical Methods in Geomechanics 30(8): 763–781.

McCartney, J.S. (2012) Issues Involved in using Temperature to Improve the Mechanical Behavior of Unsaturated Soils. Unsaturated Soils: Theory and Practice 2011, Proceedings of 5th Asia-Pacific Unsaturated Soils Conference. Jotisankasa, Sawangsuriya, Soralump and Mairaing (Editors). Kasetsart University, Thailand. pg. 509-514.

McCartney JS, Jensen E, and Counts B (2013) Measurement of the impact of volume change on thermal conductivity of subgrade soils. TRB 2013 Washington, DC January 13-17, 2013.

McCartney JS and Murphy KD (2012) Strain distributions in full-scale energy foundations. DFI Journal 6(2): 28-36.

McCartney JS and Rosenberg JE (2011) Impact of heat exchange on the axial capacity of thermo-active foundations. GeoFrontiers 2011 Dallas, TX 10 pg.

McGinley JM (1983) The Effects of Temperature on the Consolidation Process of Saturated Fine-Grained Soils. M.S. Thesis, Department of Civil, Environmental and Architectural Engineering University of Colorado Boulder.

McKinstry HA (1965) Thermal expansion of clay minerals. The American Mineralogist 50: 212–222.

Mitchell JK and Soga K (2005) Fundamentals of Soil Behavior. John Wiley & Sons, Inc. 3rd ed. New Jersey.

Omer AM (2008) Ground-source heat pumps systems and applications. Renewable and Sustainable Energy Reviews 12(2): 344-371.

Paaswell RE (1967) Temperature effects on clay soil consolidation. Journal of the Soil Mechanics and Foundation Engineering Division ASCE 93(SM3): 9–22.

Plum RL and Esrig MI (1969) Some temperature effects on soil compressibility and pore water pressure. In Effects of Temperature and Heat on Engineering Behavior of Soils. Highway Research Board, Washington, DC. Special Report, No. 103: 231–242.

Romero E, Gens A, and Lloret A (2003) Suction effects on a compacted clay under non-isothermal conditions. Géotechnique 53(1): 65–81.

Saix C, Devillers P, and El Youssoufi M.S. (2000) Element de couplage thermomechanique dans la consolidation de sols non satures. Canadian Geotechnical Journal 37(2): 308-317.

Slegel DL and Davis LR (1977) Transient heat and mass transfer in soils in the vicinity of heated porous pipes. Journal of Heat Transfer 99: 541–621.

Stewart MA (2012) Centrifuge modeling of strain distributions in energy foundations. MS Thesis. University of Colorado Boulder. 110 pg.

Sultan N, Delage P, and Cui Y-J (2002) Temperature effects on the volume change behavior of Boom clay. Engineering Geology 64: 135–145.

Tang A-M and Cui Y-J (2009) Modelling the thermomechanical volume change behaviour of compacted expansive clays. Géotechnique 59(3): 185–195.

Towhata I, Kuntiwattanakul P, Seko I, and Ohishi K (1993) Volume change of clays induced by heating as observed in consolidation tests. Soils and Foundations 33(4): 170–183.

Uchaipichat A, and Khalili N (2009) Experimental investigation of thermo-hydro-mechanical behaviour of an unsaturated silt. Géotechnique 59(4): 339–353.

Vega A, Coccia CJR, El Tawati A, McCartney JS (2012) Impact of the rate of heating on the thermal consolidation of saturated silt. GeoCongress 2012 ASCE Oakland CA March 25-29th 2012 10 pg.

Table captions.

Table 1. Initial void ratio and stress states for the compacted silt specimens

Figure captions.

Figure 1. Applicability of thermal volume changes on soil-structure interaction in energy foundations

Figure 2. Characteristics of Bonny silt: (a) Grain size distribution; (b) Compaction curves; (c) Thermal conductivity

Figure 3. Experimental setup: (a) Schematic of the thermal oedometer cell; (b) Picture of the thermal oedometer cell and load frame

Figure 4: Mechanical machine deflections of the oedometer system

Figure 5. Thermal deflections of the oedometer system: (a) Measured and corrected values; (b) Thermal axial displacement versus strain

Figure 6. Schematic representation of the testing sequences for the five thermal consolidation tests with cyclic heating and cooling

Figure 7. Compression curves obtained during application of different stress states to saturated Bonny silt specimens

Figure 8. Typical time series of the different measurements during the test on the normally consolidated specimen: (a) Temperature and axial stress in the first 10000 s of the first heating-cooling cycle; (b) Vertical displacements and pore water pressure in the first 10000 s of the first heating-cooling cycle; (c) Temperature and axial stress during all heating-cooling cycles; (d) Vertical displacements and pore water pressure during all heating-cooling cycles

Figure 9: Axial strain as a function of changes in temperature for different initial stress states: (a) OCR 1.00; (b) OCR 1.28; (c) OCR 1.80; (d) OCR 7.36; (e) OCR 30.29

Figure 10: Permanent axial strain after temperature cycles with $\Delta T \approx 75$ °C: (a) Permanent strain as a function of heating cycles for different OCRs; (b) Permanent strain as a function of OCR for different numbers of heating cycles; (c) Permanent strain normalized by the change in temperature for different numbers of heating cycles

Table 1. Initial void ratio and stress states for the compacted silt specimens

Test number	$e_{compaction}$	$w_{compaction}$ (%)	$\sigma'_{preconsol.}$ (kPa)	$\sigma'_{initial}$ (kPa)	OCR	$e_{initial}$
1	0.657	15.1	1195.4	1195.4	1.00	0.516
2	0.667	15.3	1203.6	940.2	1.28	0.506
3	0.662	15.2	1199.1	666.1	1.80	0.511
4	0.660	15.3	1162.6	158.0	7.36	0.549
5	0.661	15.3	1197.9	39.5	30.29	0.559

Figure 1
Click here to download high resolution image

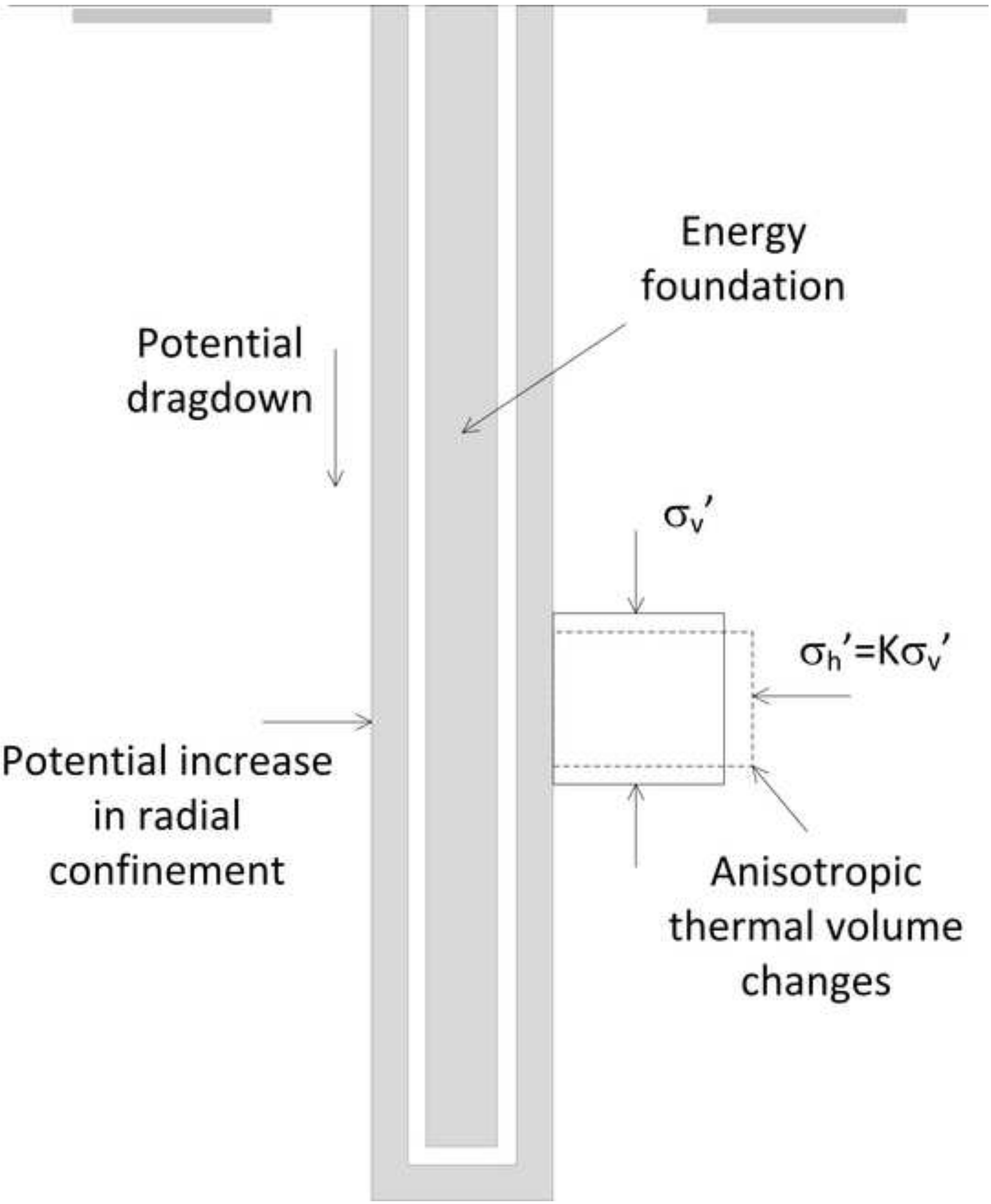

Figure 2 (old, use excel)

Click here to download high resolution image

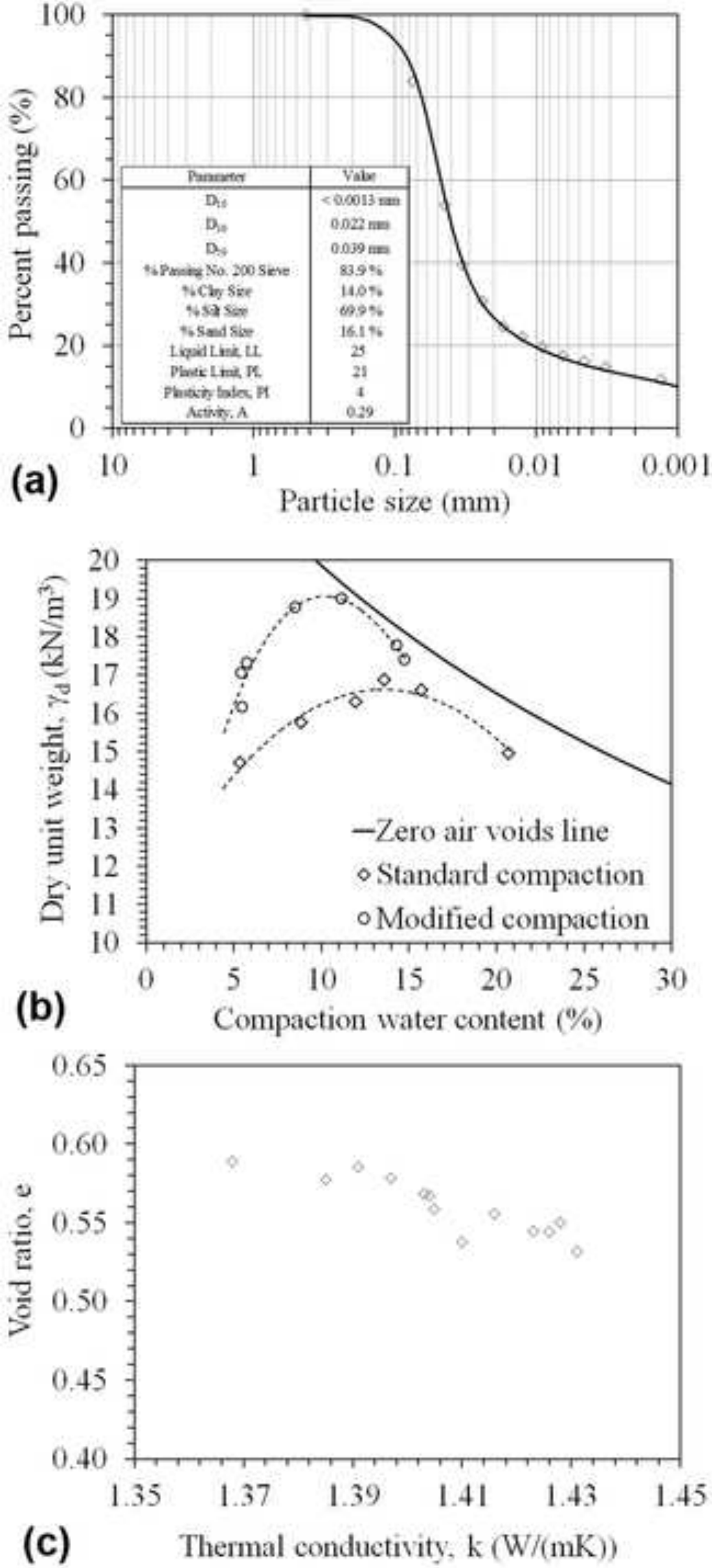

Figure 3a

Click here to download high resolution image

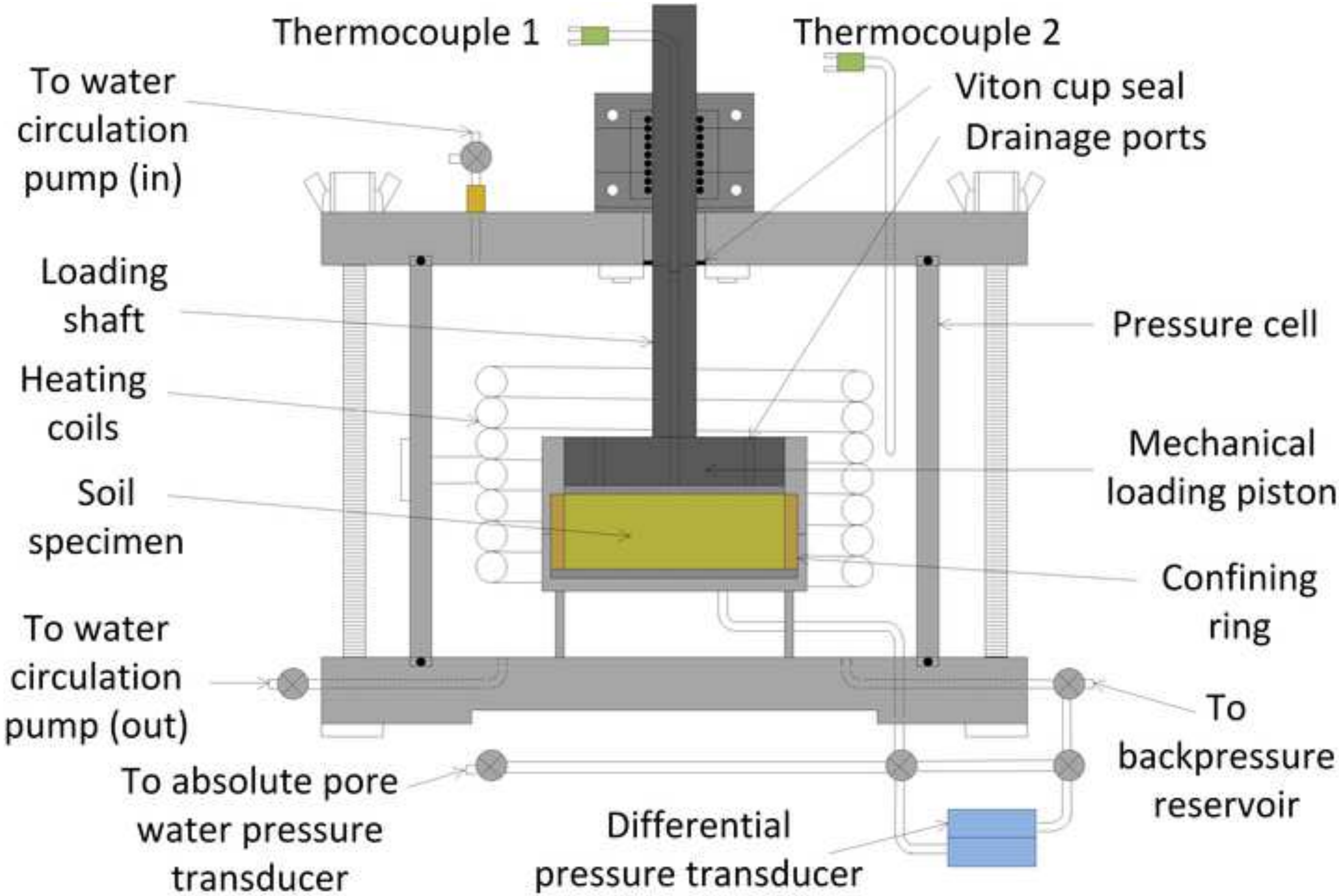

Figure 3b

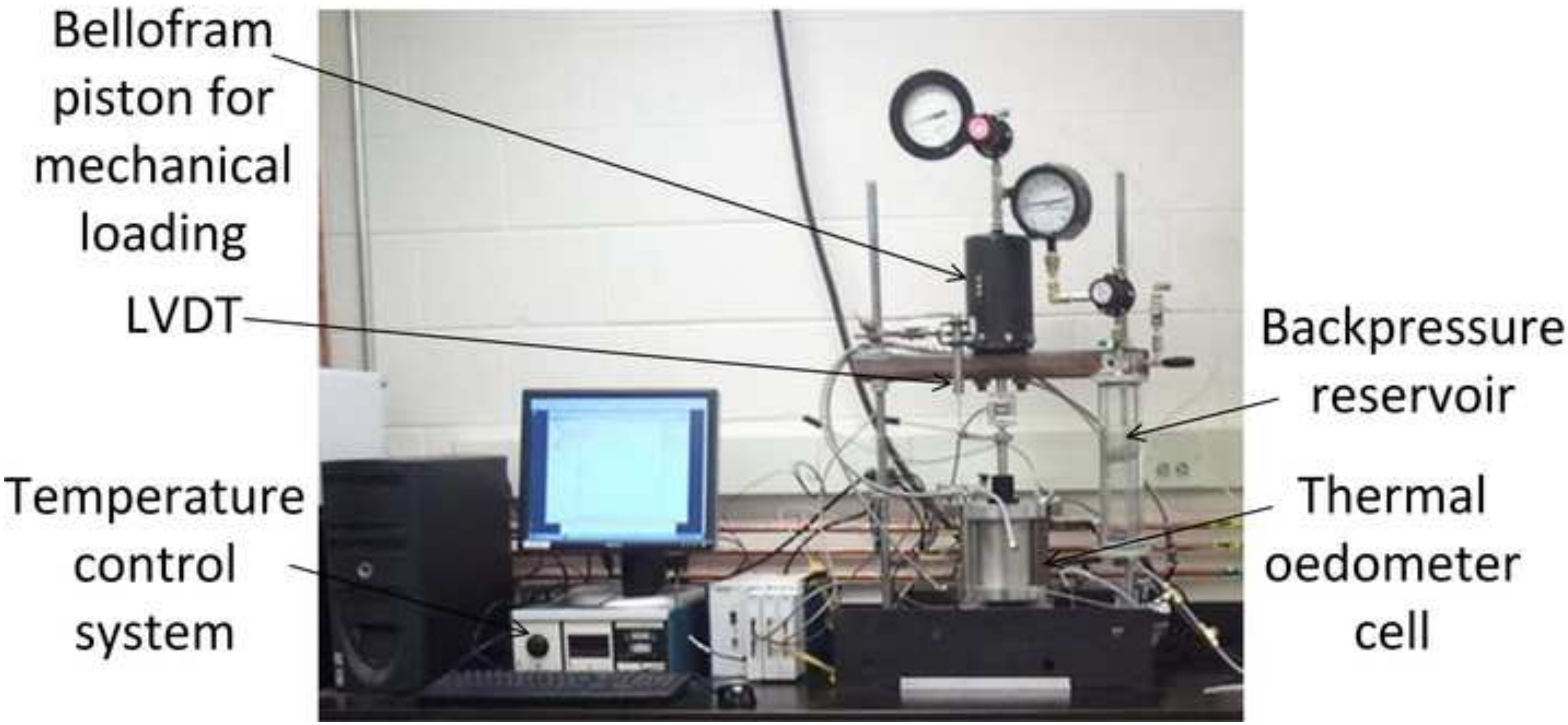
Bellofram piston for mechanical loading
LVDT
Temperature control system
Backpressure reservoir
Thermal oedometer cell

Figure 4 (old, use excel)
Click here to download high resolution image

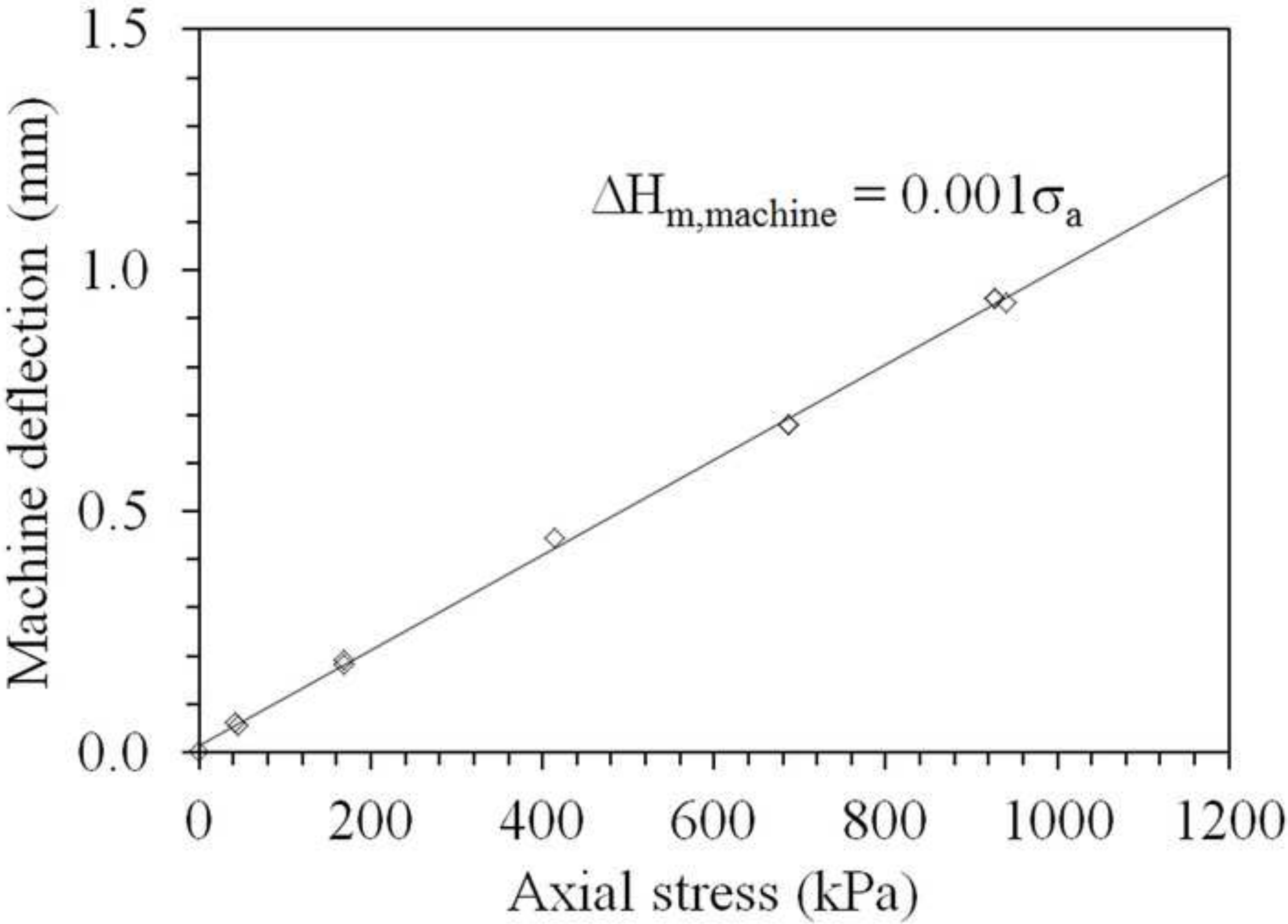

Figure 5 (old, use excel)
Click here to download high resolution image

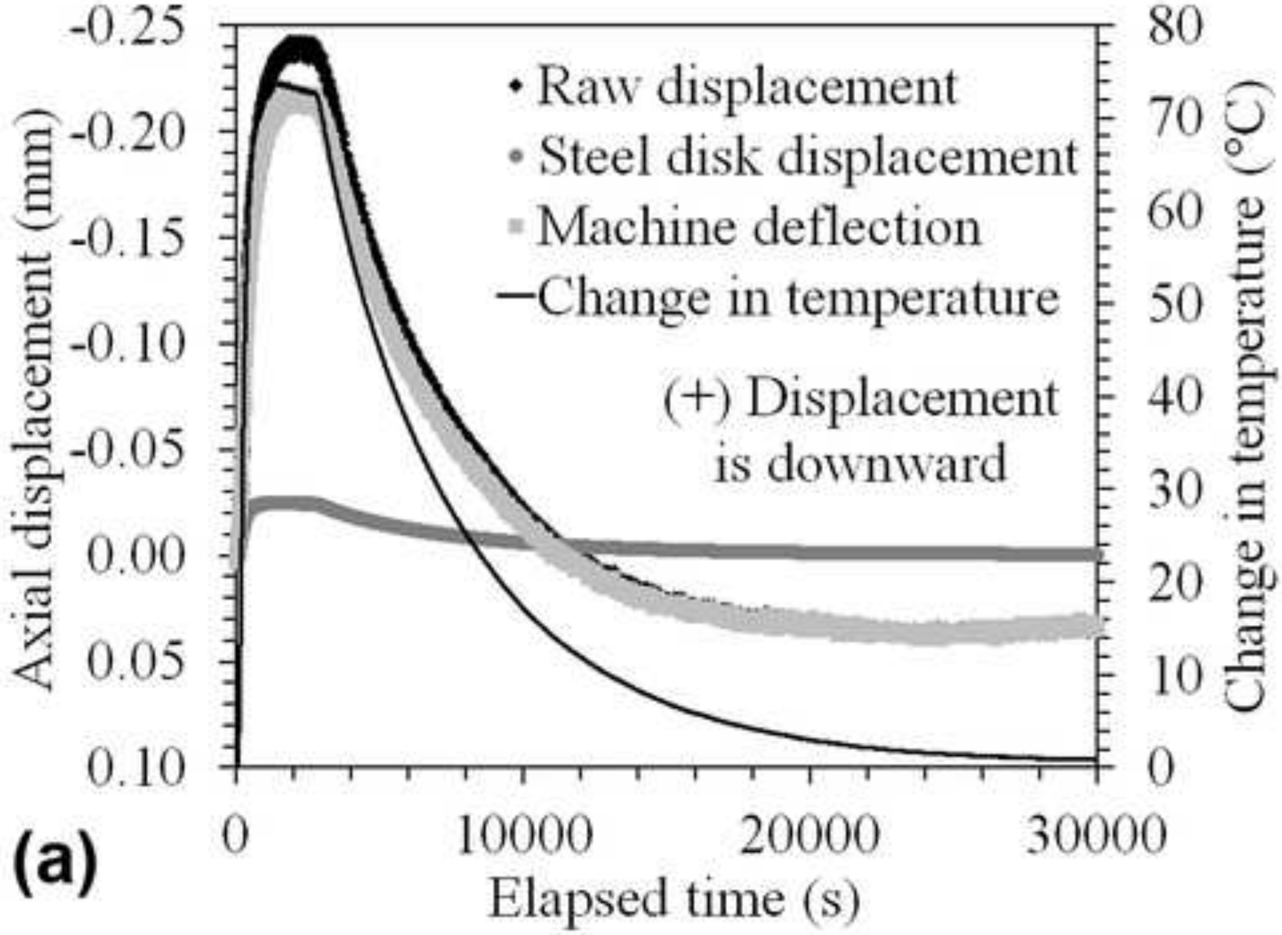

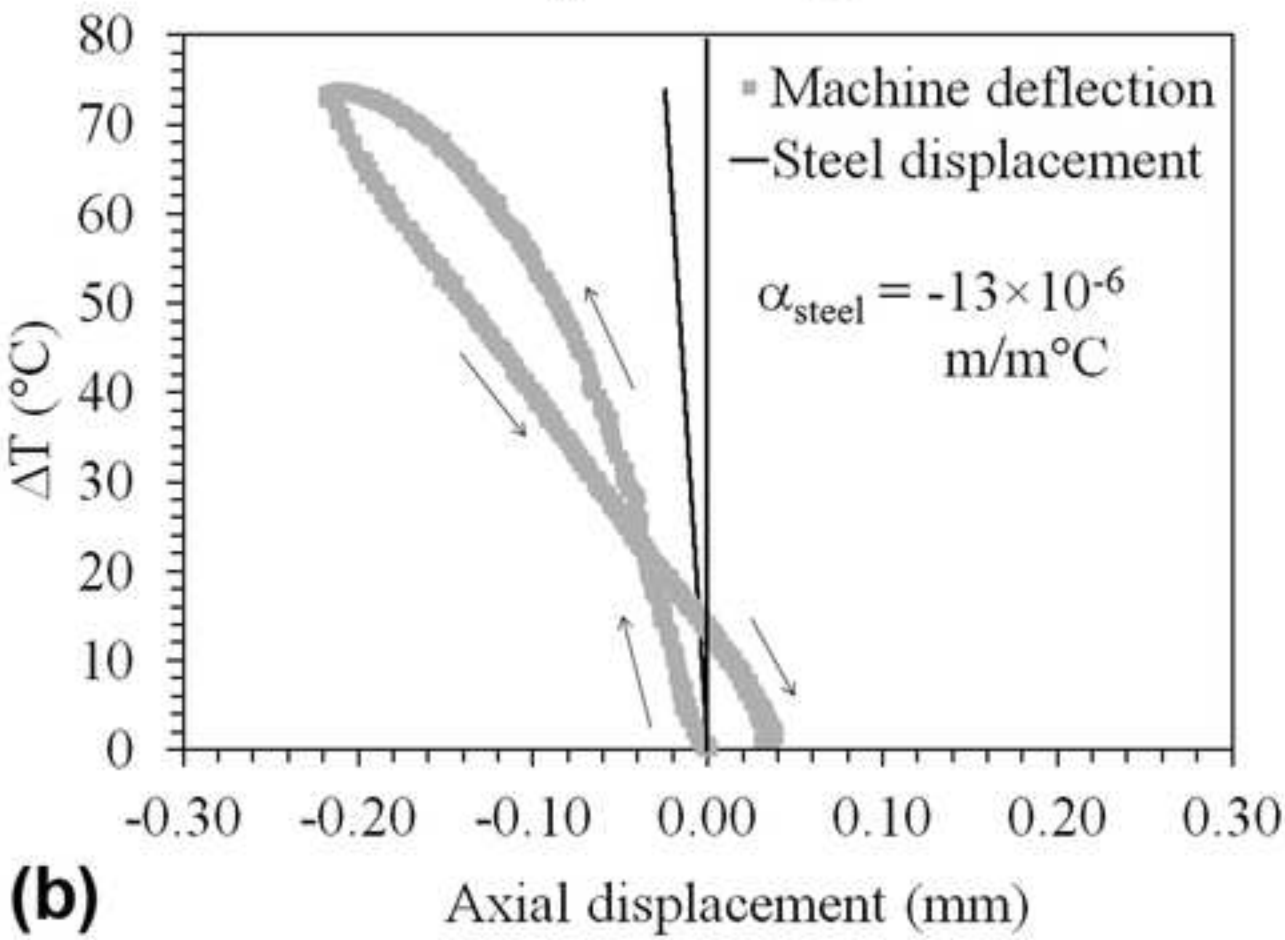

Figure 6
Click here to download high resolution image

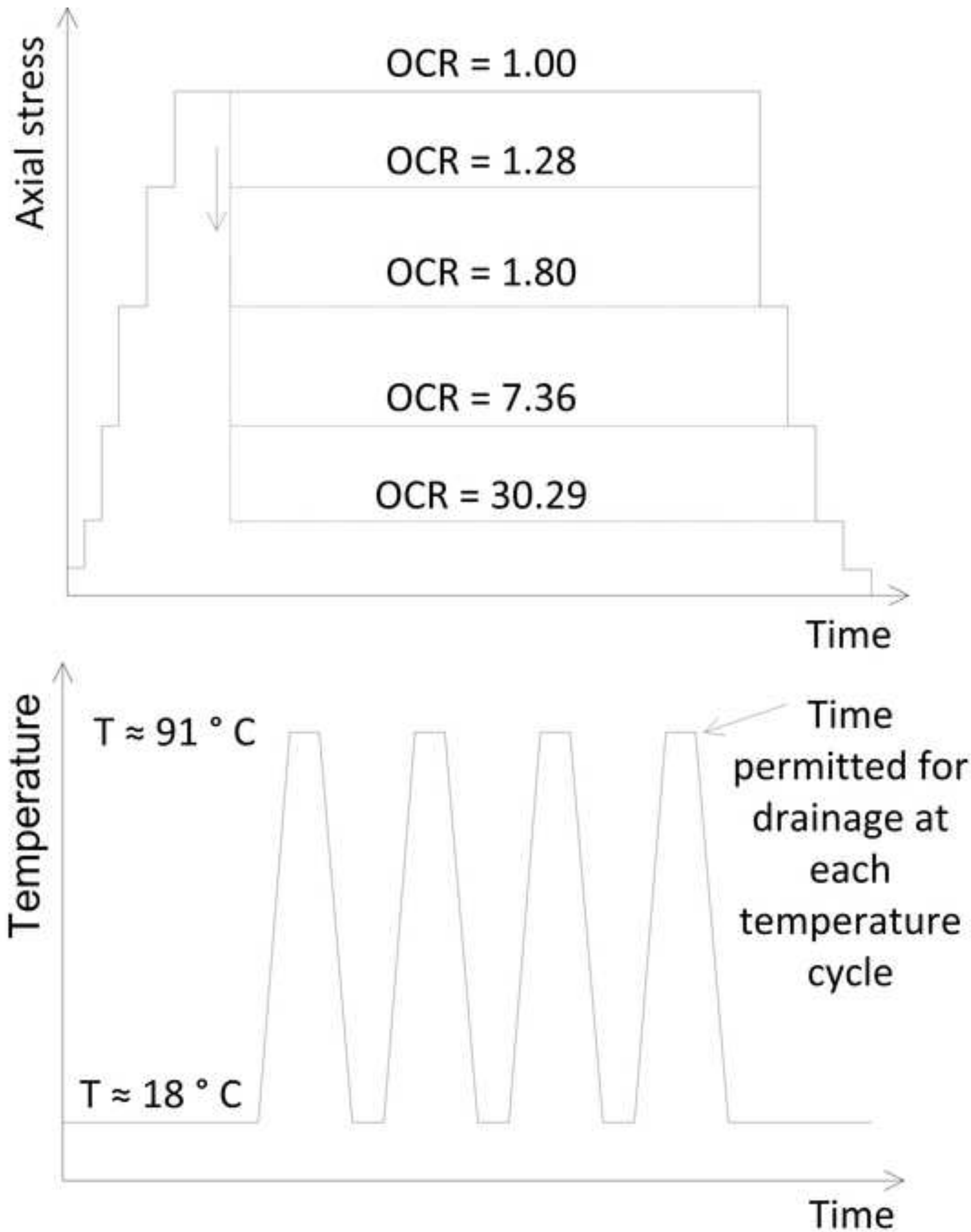

Figure 7 (old, use excel)
Click here to download high resolution image

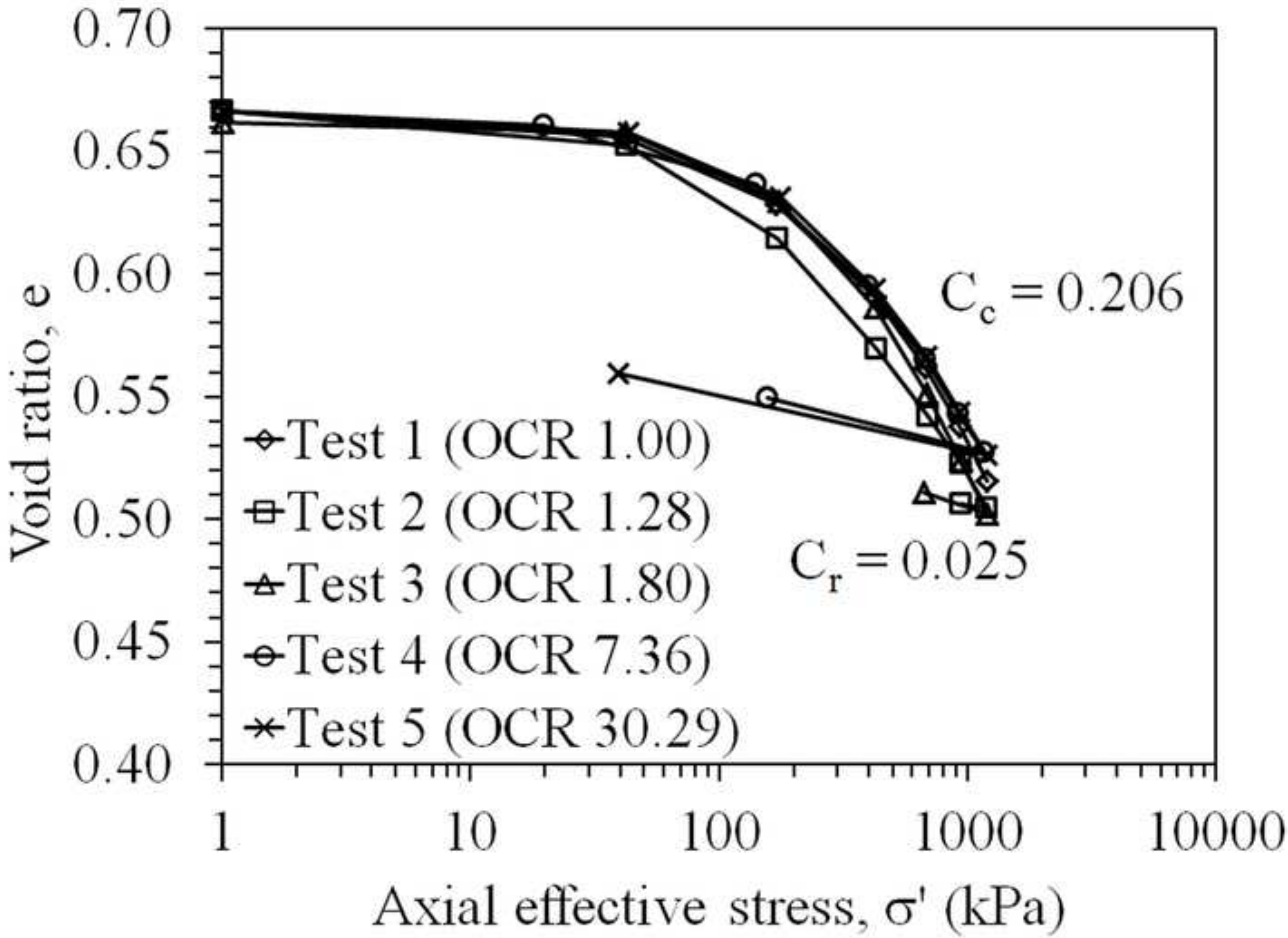

Figure 8 (old, use excel)
Click here to download high resolution image

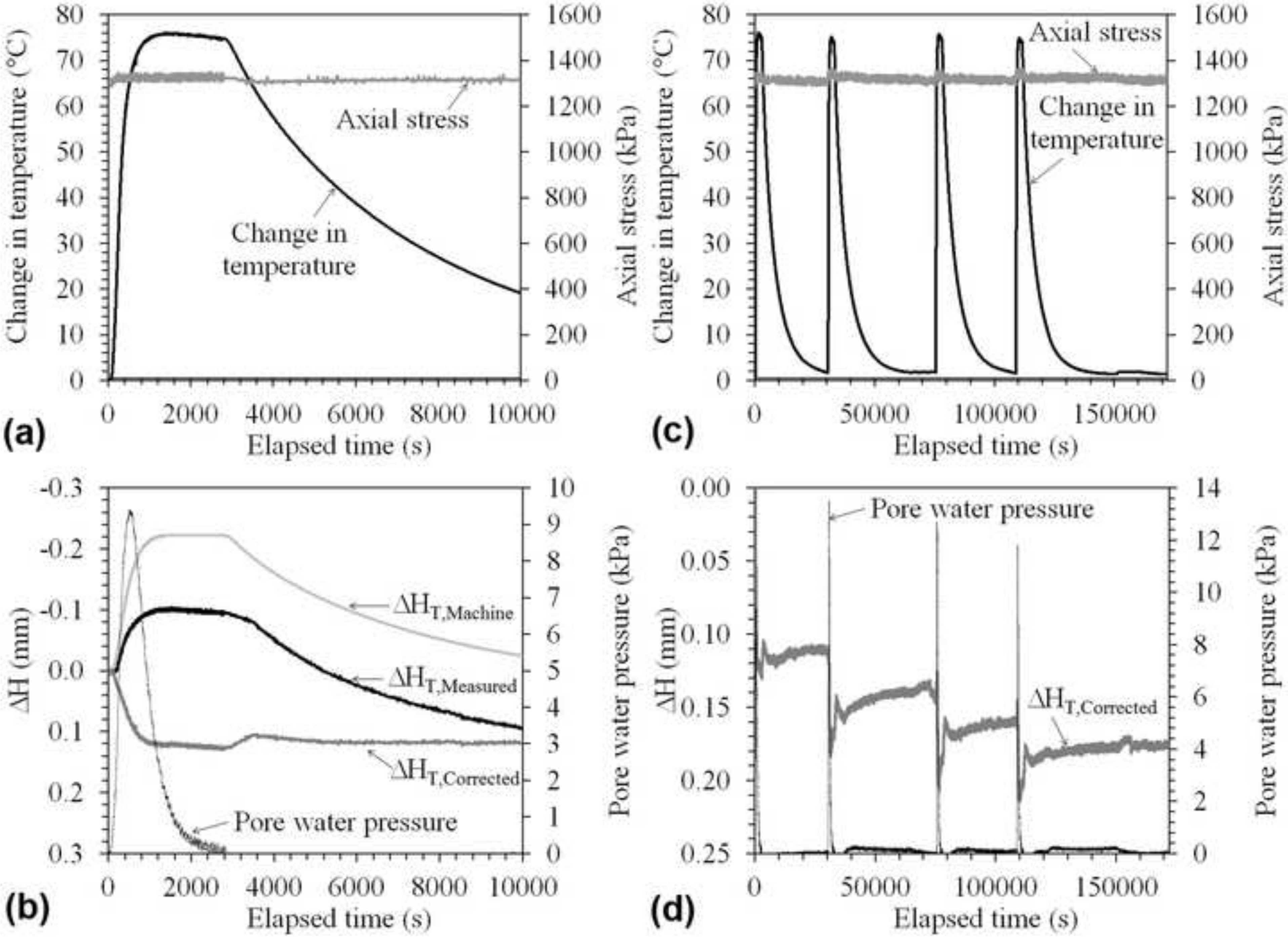

Figure 9 (old, use excel)
Click here to download high resolution image

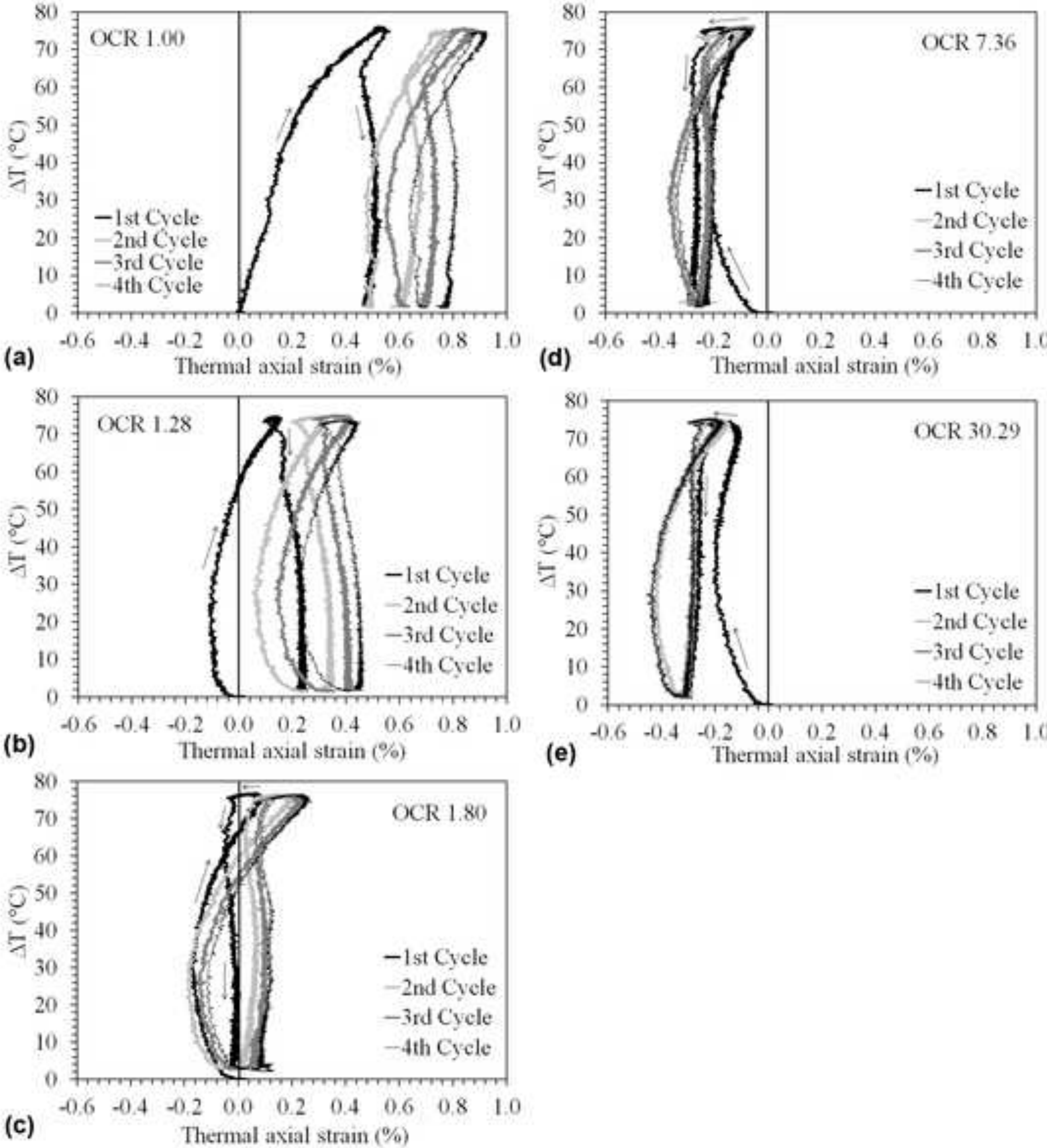

Figure 10 (old, use excel)
Click here to download high resolution image

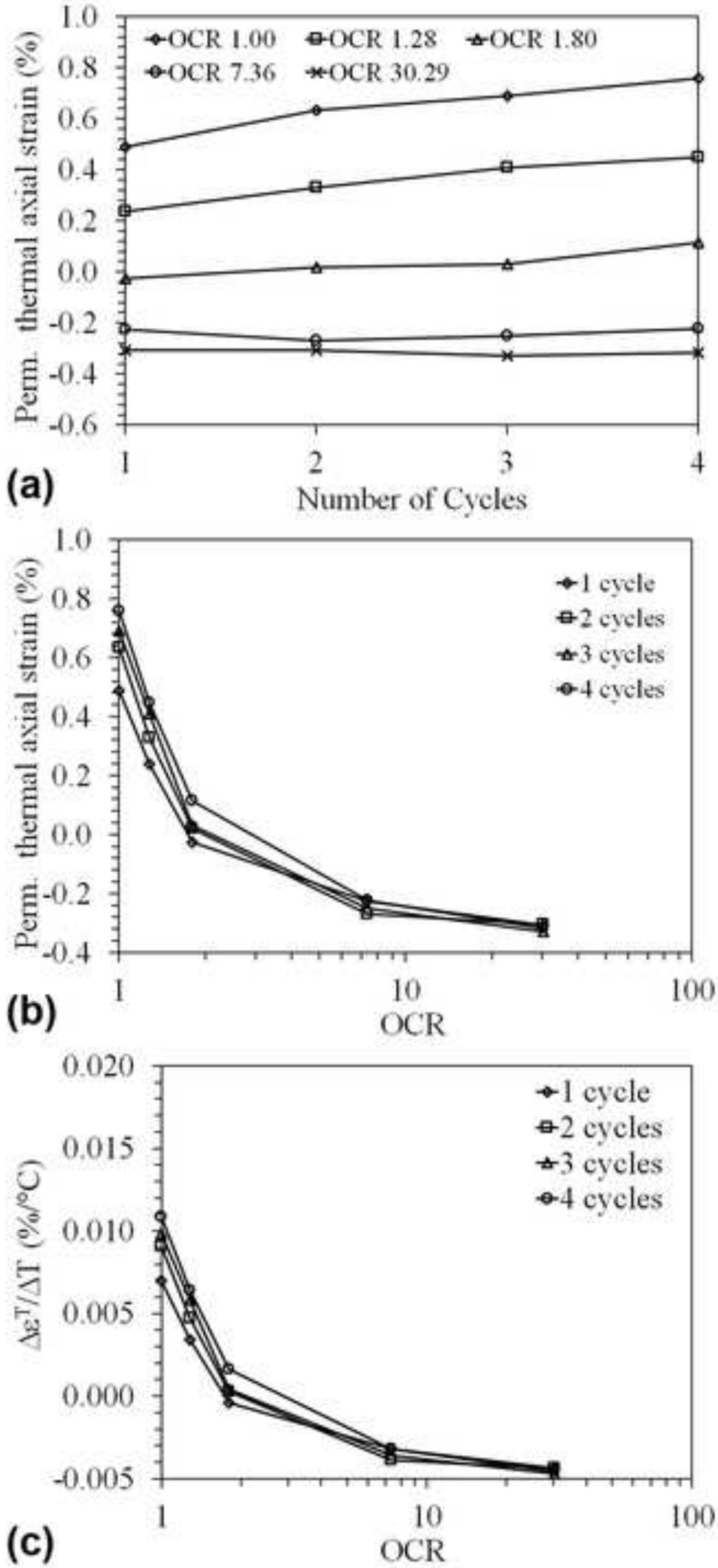

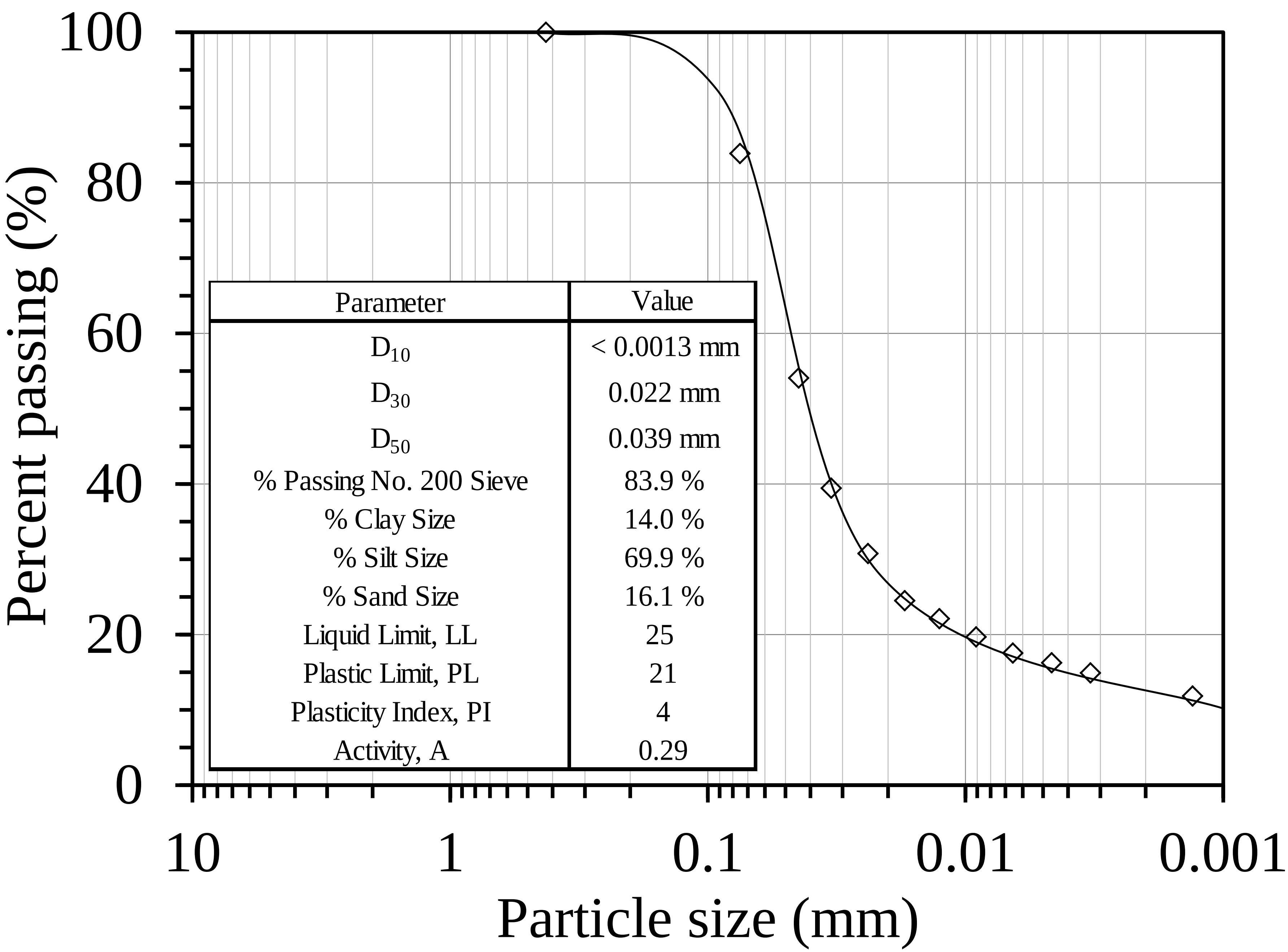

Parameter	Value
D_{10}	< 0.0013 mm
D_{30}	0.022 mm
D_{50}	0.039 mm
% Passing No. 200 Sieve	83.9 %
% Clay Size	14.0 %
% Silt Size	69.9 %
% Sand Size	16.1 %
Liquid Limit, LL	25
Plastic Limit, PL	21
Plasticity Index, PI	4
Activity, A	0.29

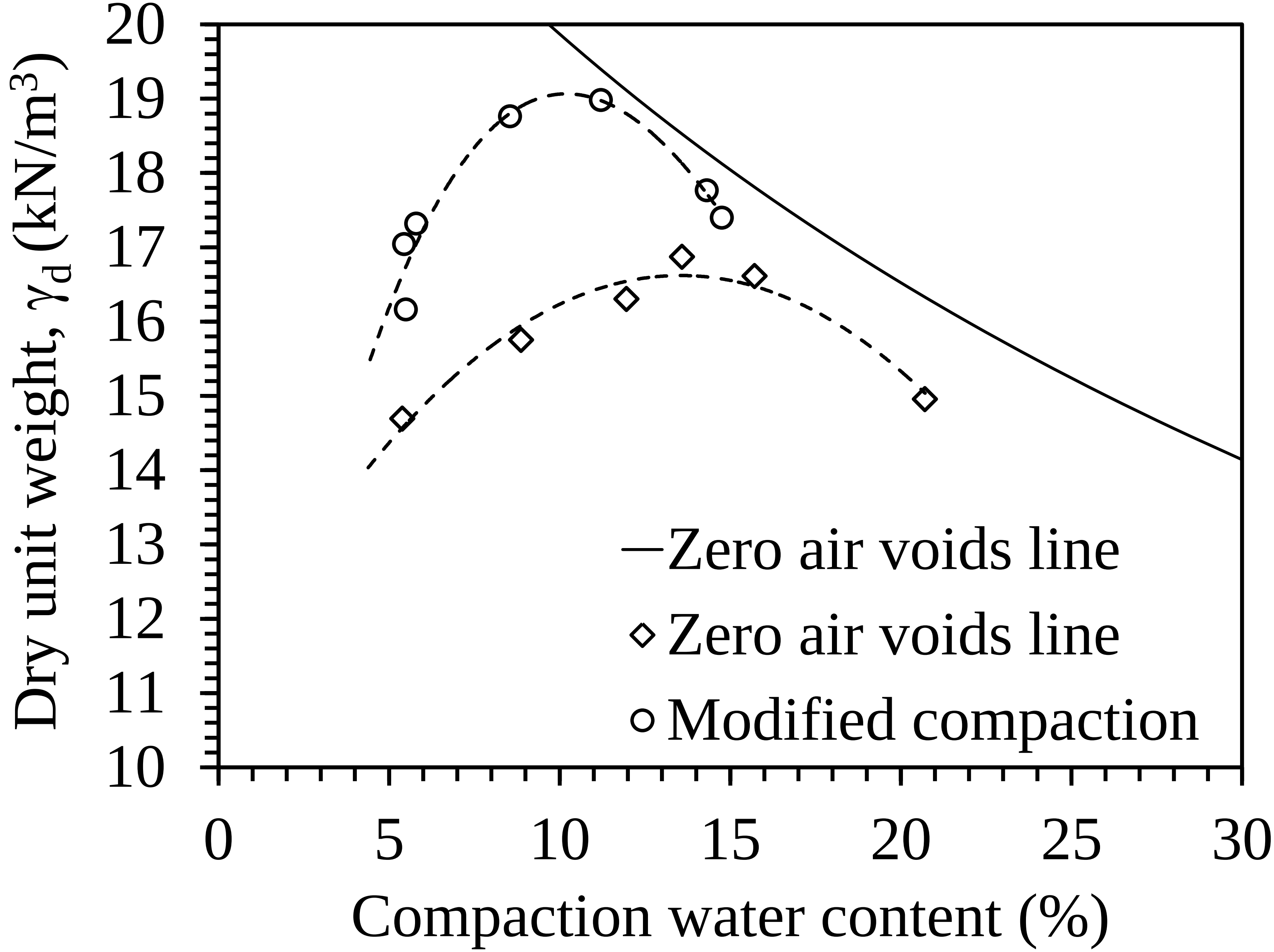

Dry unit weight, γ_d (kN/m^3)
20
19
18
17
16
15
14
13
12
11
10
0
5
10
15
20
25
30
Compaction water content (%)
Zero air voids line
Zero air voids line
Modified compaction

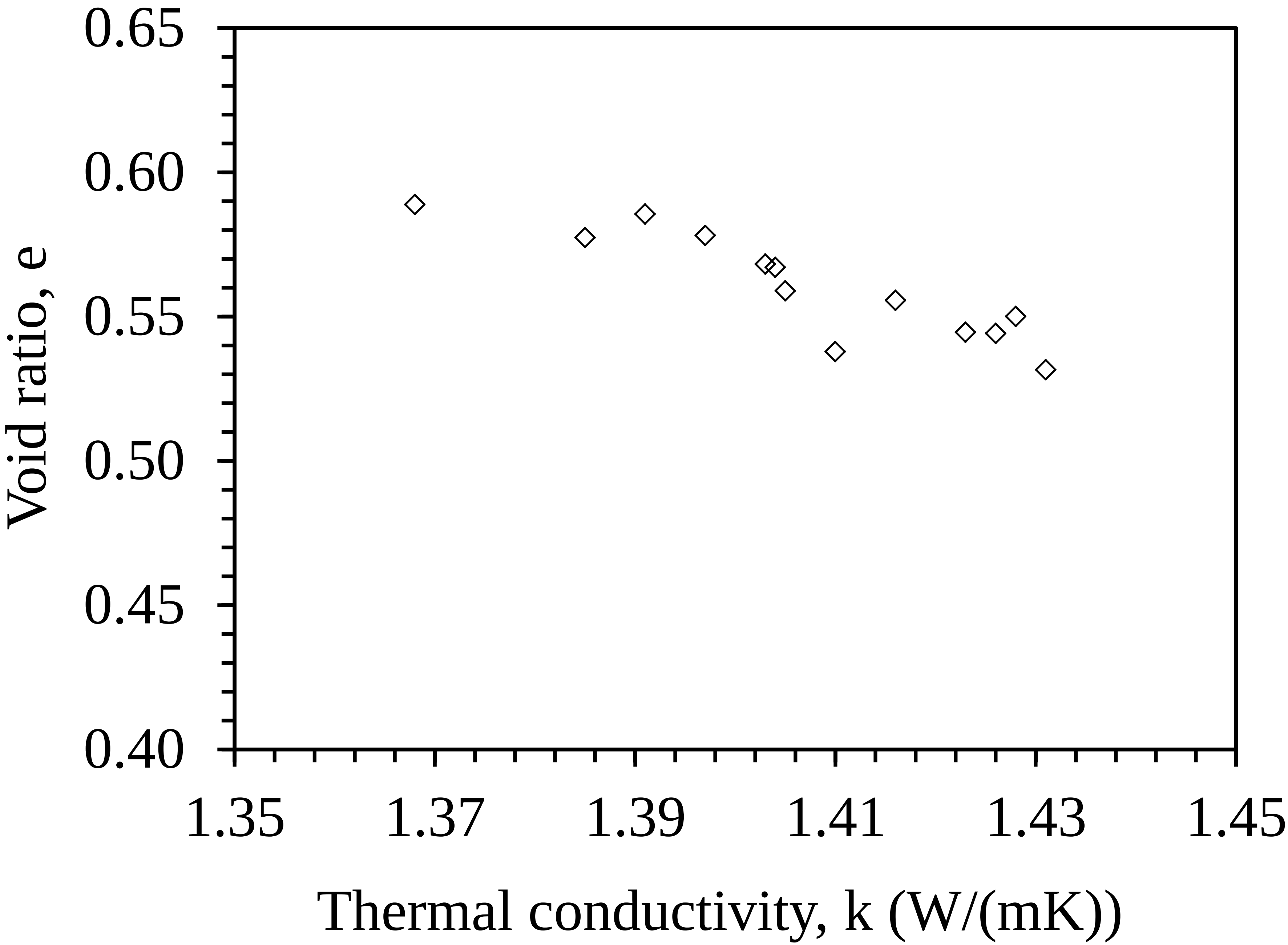
0.65
0.60
0.55
0.50
0.45
0.40
Void ratio, e
1.35
1.37
1.39
1.41
1.43
1.45
Thermal conductivity, k (W/(mK))

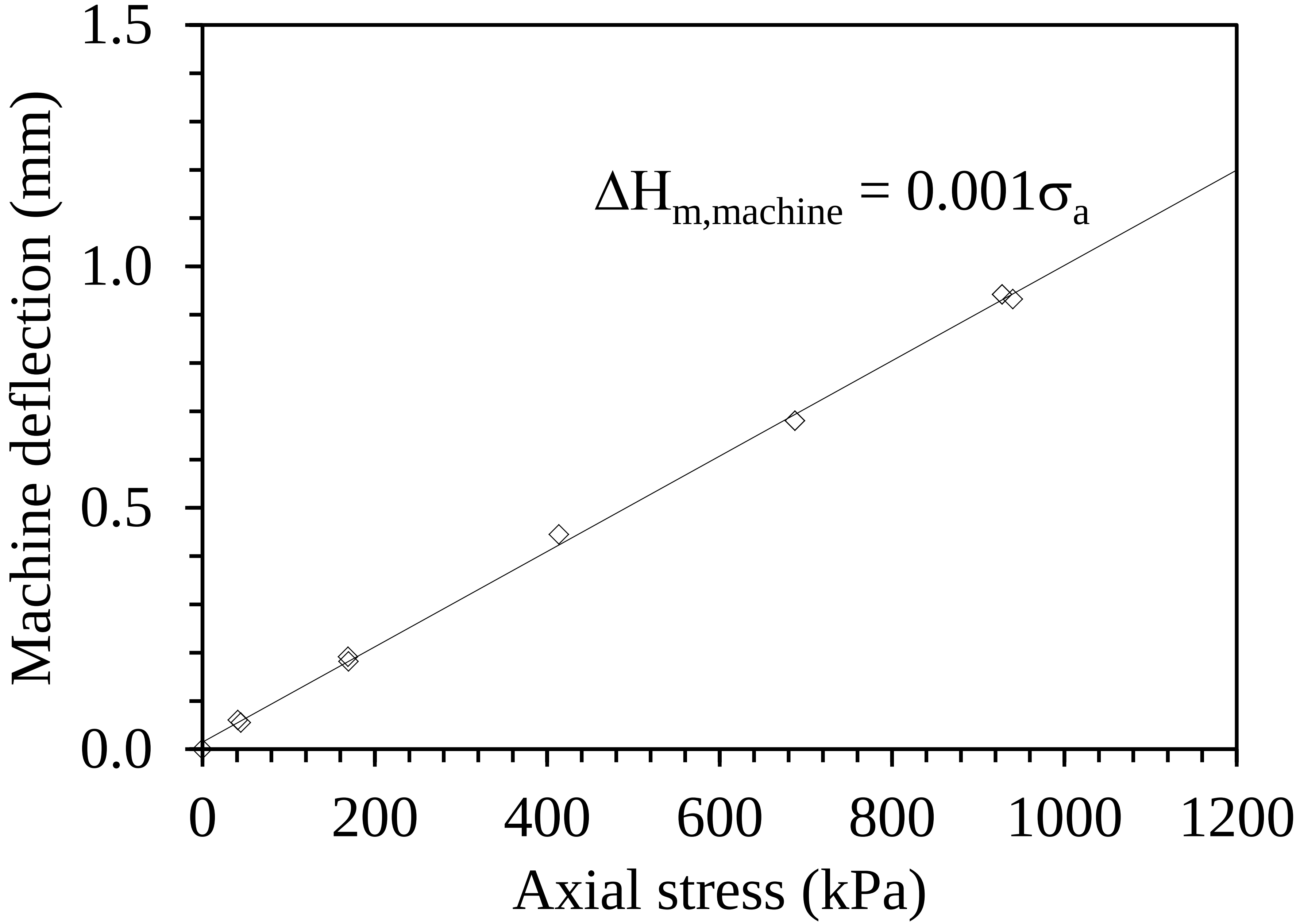

1.5
1.0
0.5
0.0
Machine deflection (mm)
ΔH_m,machine = 0.001σ_a
0
200
400
600
800
1000
1200
Axial stress (kPa)

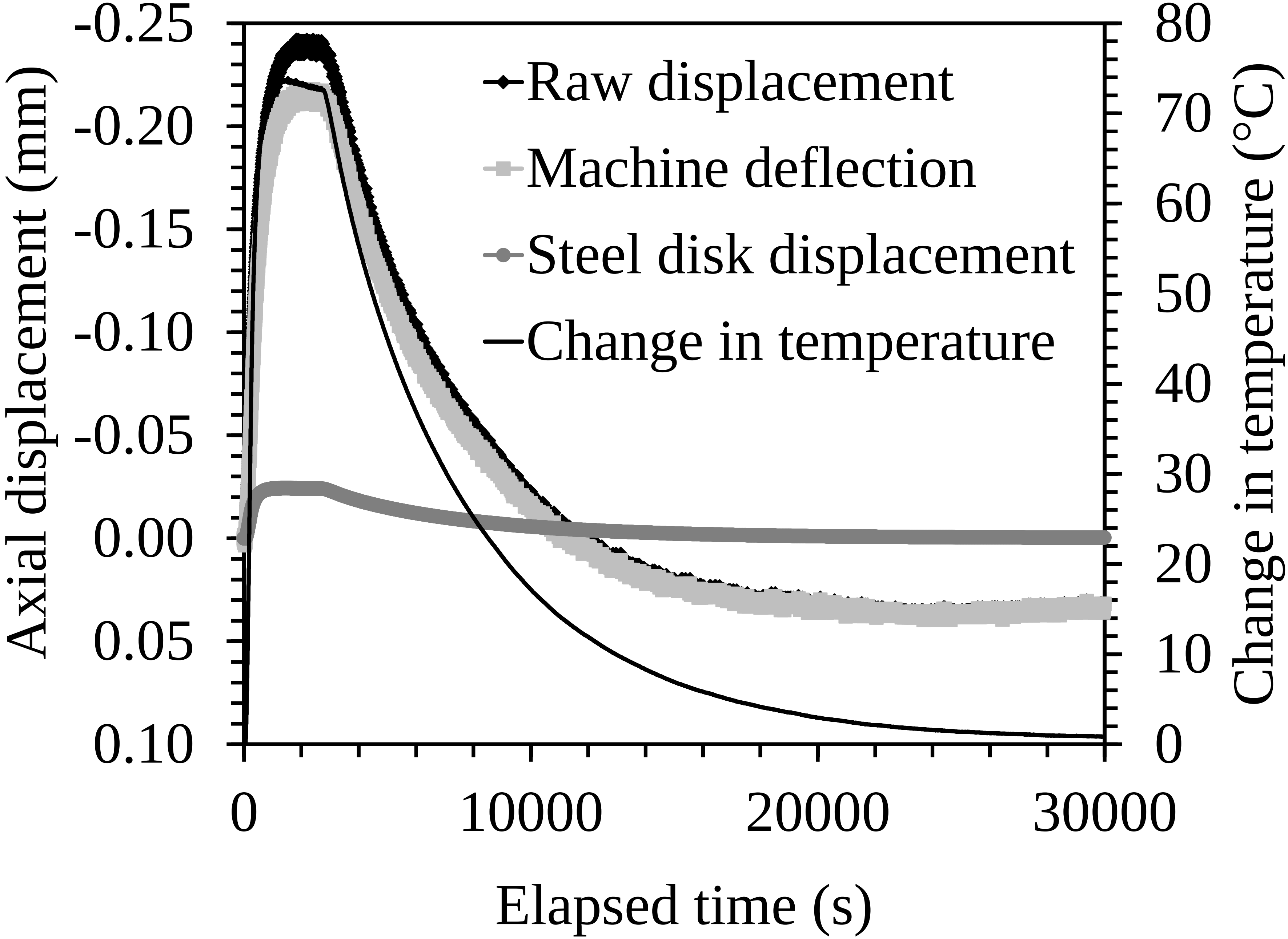

Raw displacement
Machine deflection
Steel disk displacement
Change in temperature
Axial displacement (mm)
-0.25
-0.20
-0.15
-0.10
-0.05
0.00
0.05
0.10
Change in temperature (°C)
80
70
60
50
40
30
20
10
0
0
10000
20000
30000
Elapsed time (s)

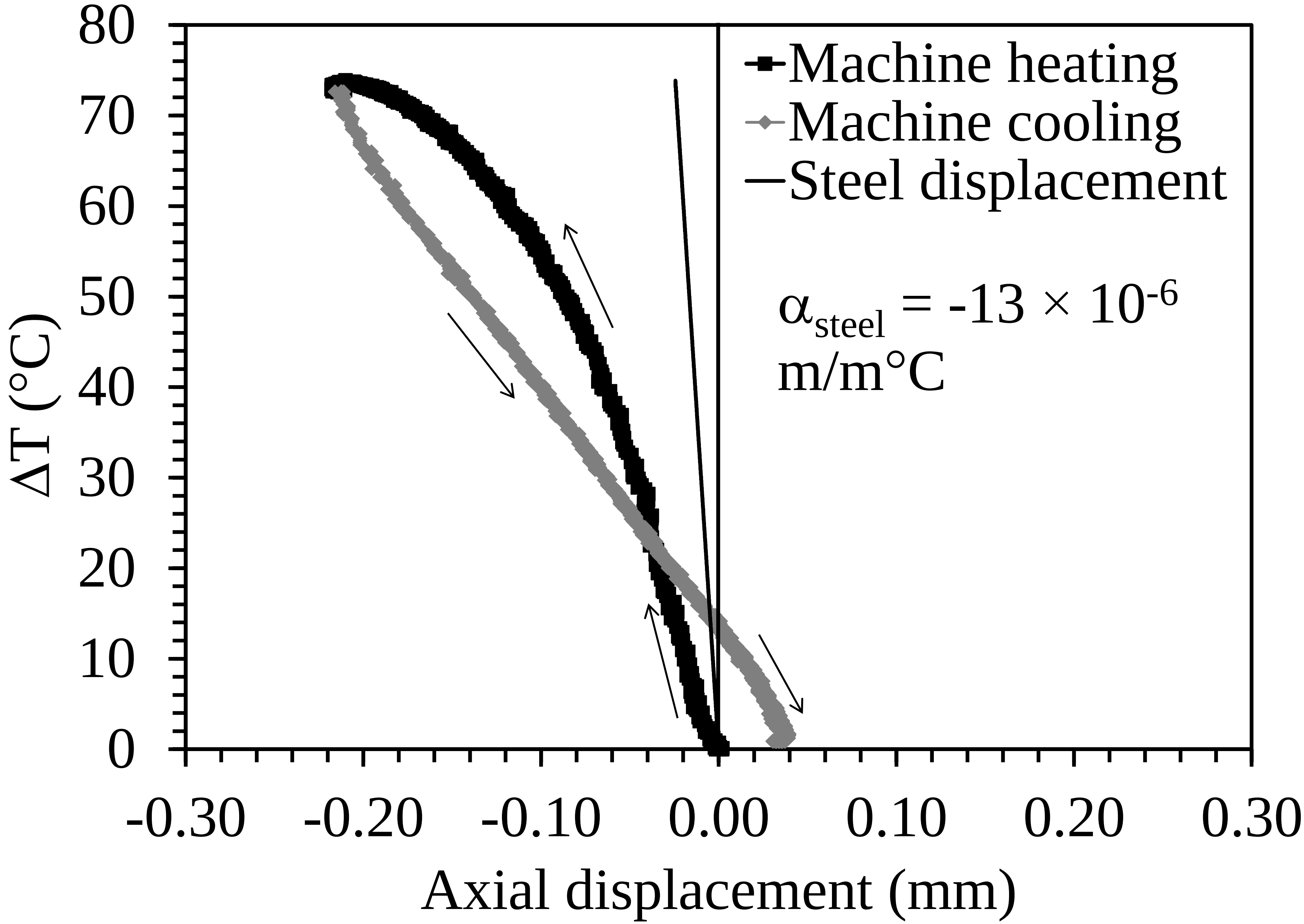

80
70
60
50
40
30
20
10
0
ΔT (°C)
-0.30
-0.20
-0.10
0.00
0.10
0.20
0.30
Axial displacement (mm)
Machine heating
Machine cooling
Steel displacement
$\alpha_{steel} = -13 \times 10^{-6}$ m/m°C

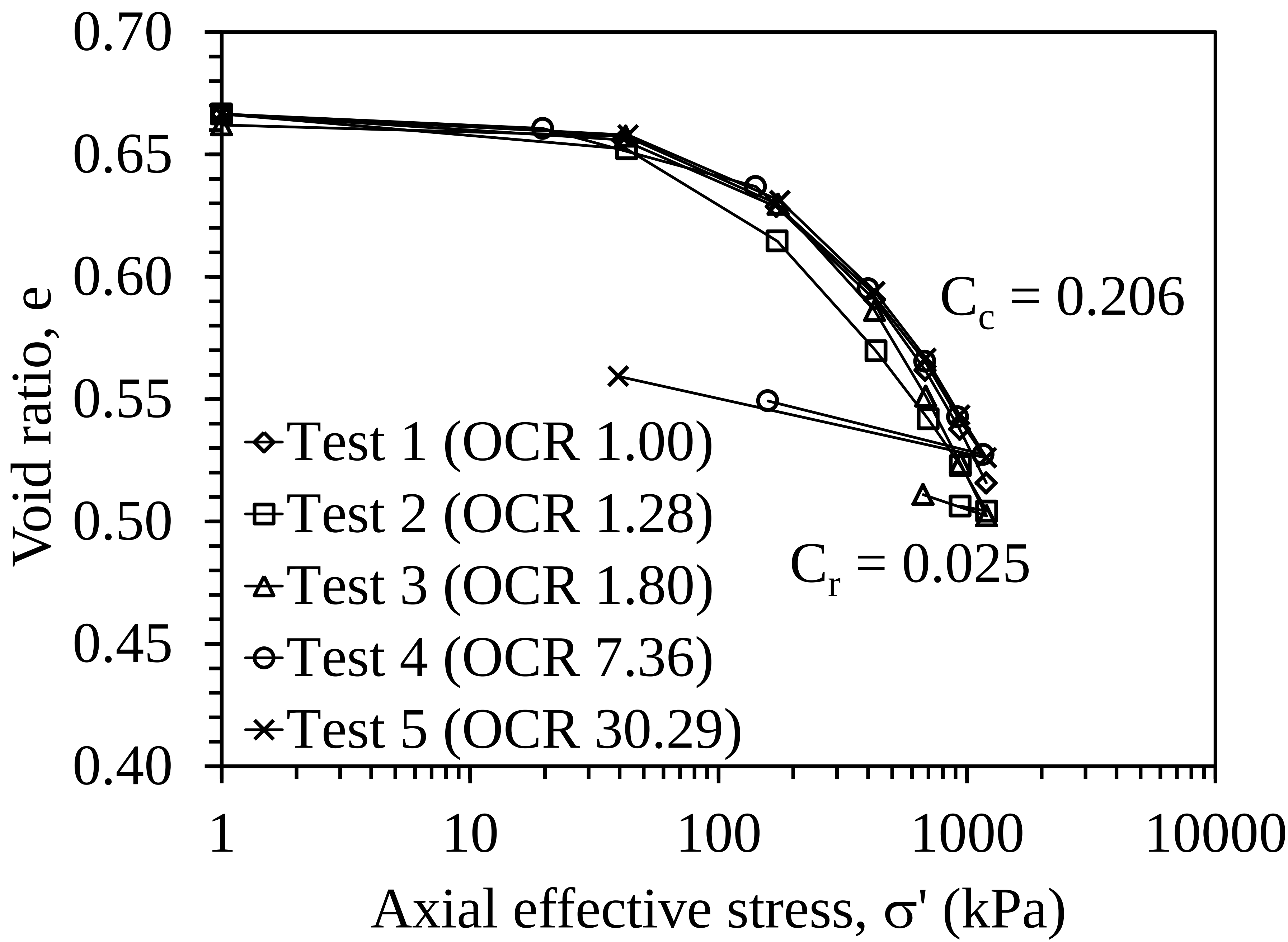

0.70
0.65
0.60
0.55
0.50
0.45
0.40
Void ratio, e
1
10
100
1000
10000
Axial effective stress, σ' (kPa)
Cc = 0.206
Cr = 0.025
Test 1 (OCR 1.00)
Test 2 (OCR 1.28)
Test 3 (OCR 1.80)
Test 4 (OCR 7.36)
Test 5 (OCR 30.29)

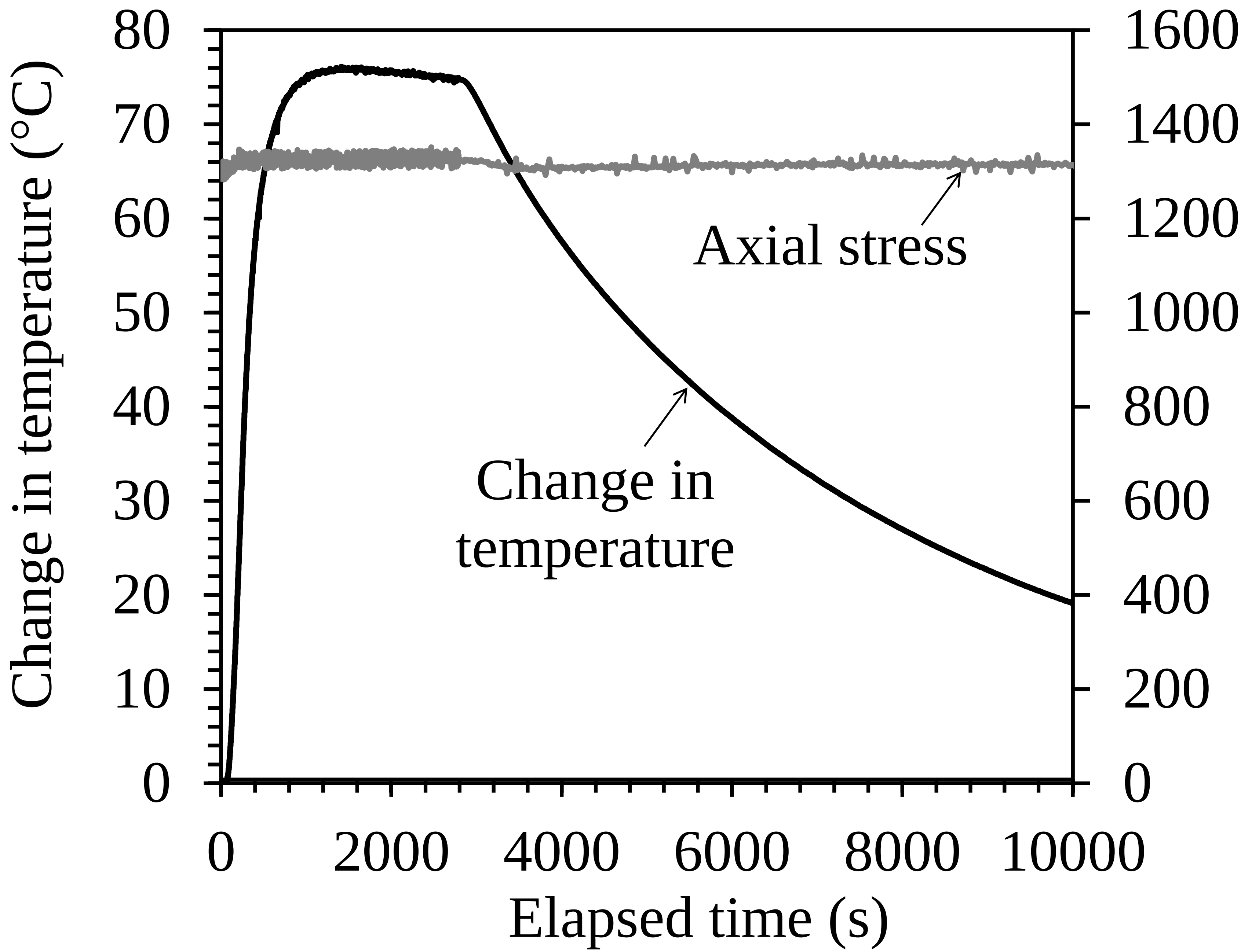

Change in temperature (°C)
Axial stress (kPa)
Elapsed time (s)
Axial stress
Change in temperature
0
10
20
30
40
50
60
70
80
0
200
400
600
800
1000
1200
1400
1600
0
2000
4000
6000
8000
10000

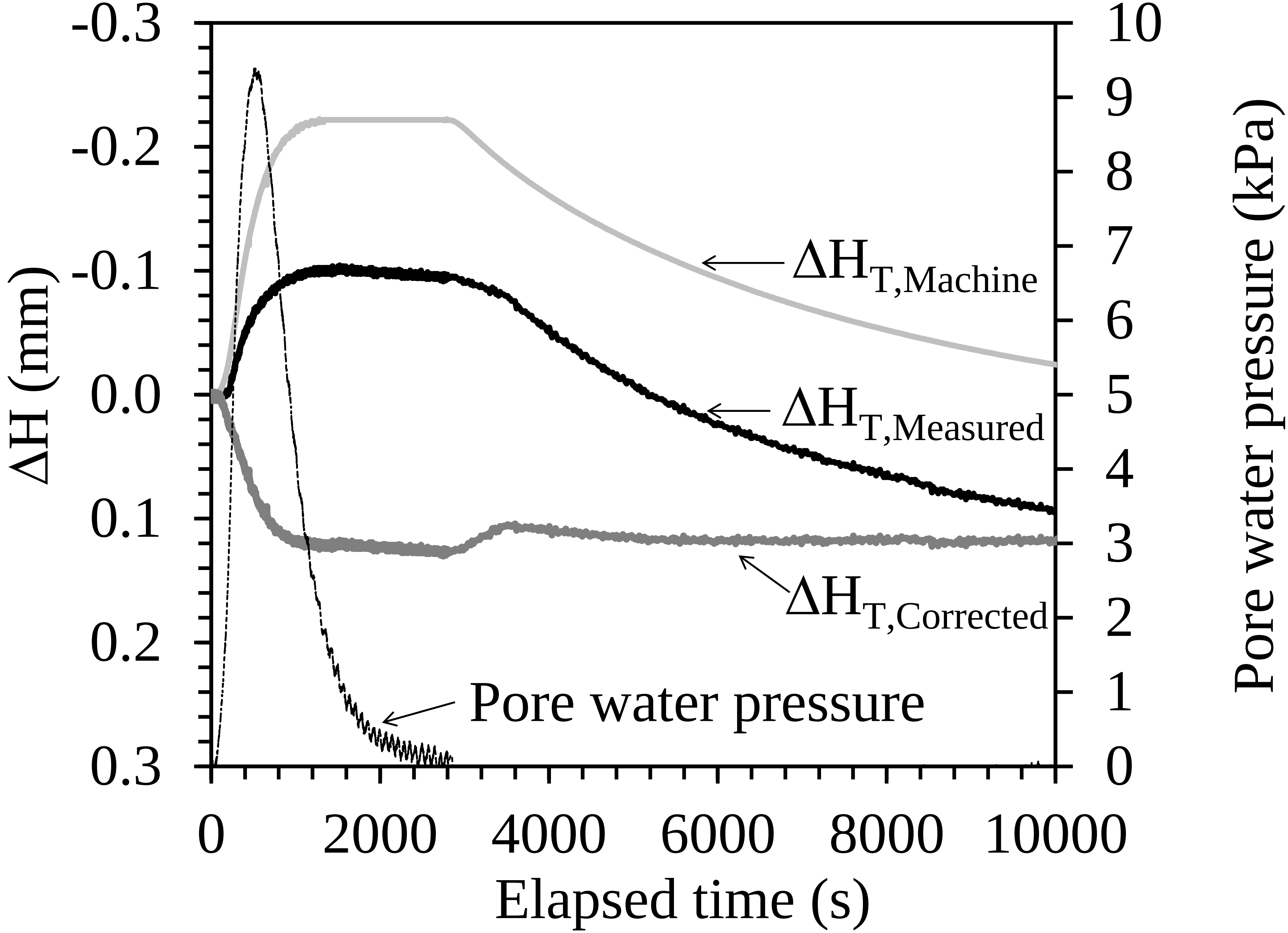

-0.3
-0.2
-0.1
0.0
0.1
0.2
0.3
ΔH (mm)
10
9
8
7
6
5
4
3
2
1
0
Pore water pressure (kPa)
0
2000
4000
6000
8000
10000
Elapsed time (s)
ΔH_T,Machine
ΔH_T,Measured
ΔH_T,Corrected
Pore water pressure

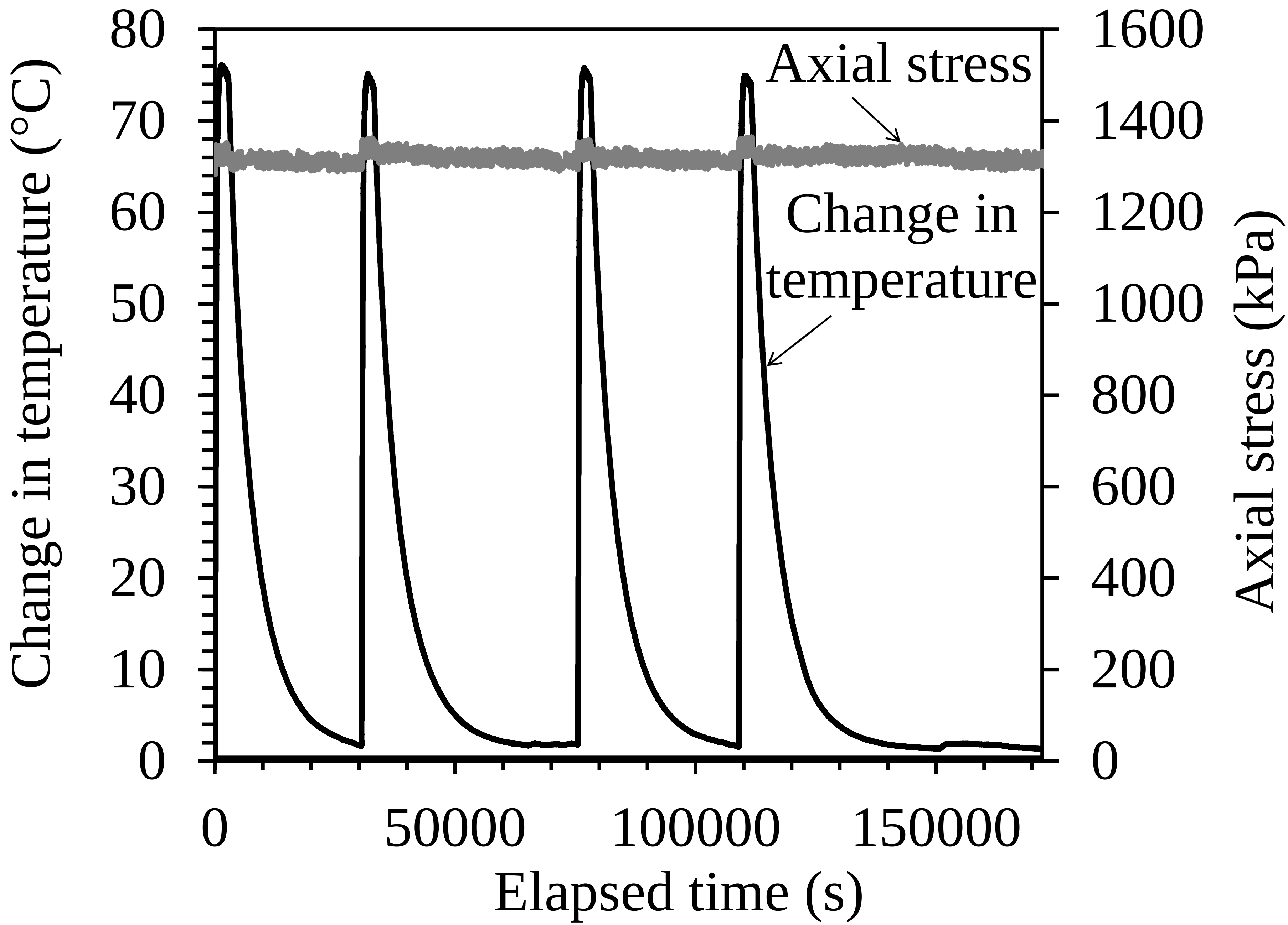
80
70
60
50
40
30
20
10
0
1600
1400
1200
1000
800
600
400
200
0
Axial stress
Change in
temperature
Change in temperature (°C)
Axial stress (kPa)
0
50000
100000
150000
Elapsed time (s)

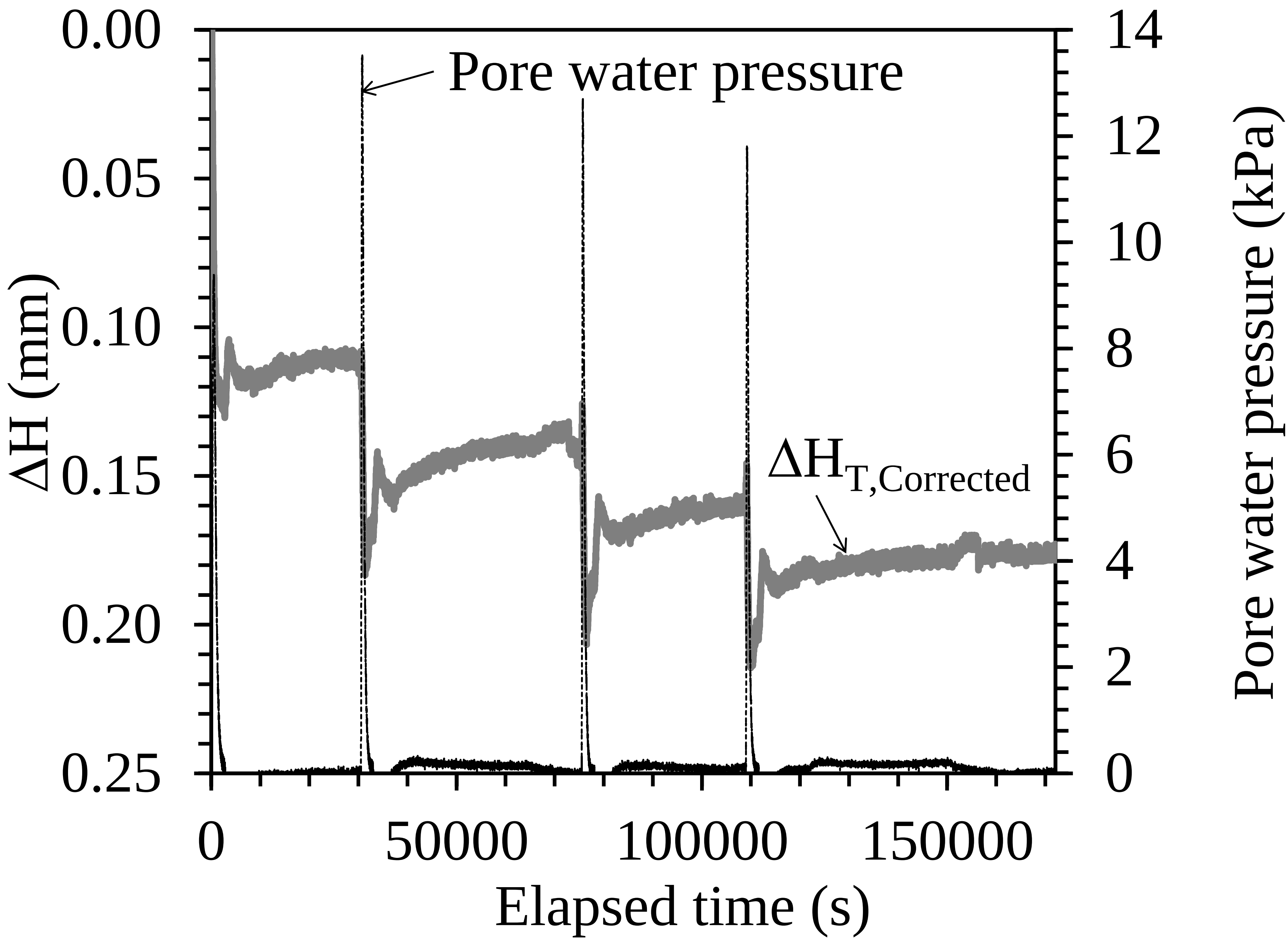

Pore water pressure
$\Delta H_{T,Corrected}$
0.00
0.05
0.10
0.15
0.20
0.25
ΔH (mm)
14
12
10
8
6
4
2
0
Pore water pressure (kPa)
0
50000
100000
150000
Elapsed time (s)

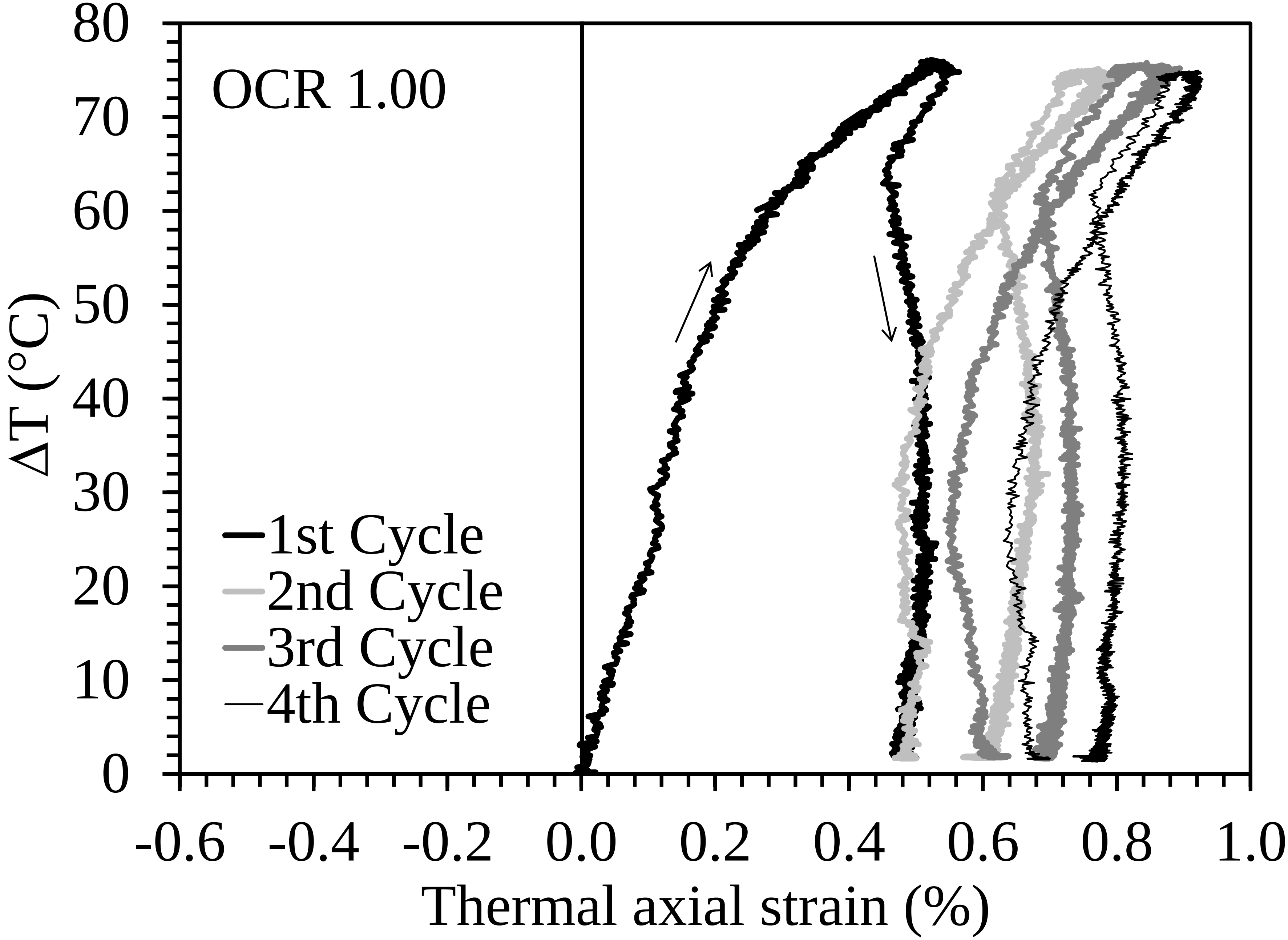

OCR 1.00
ΔT (°C)
80
70
60
50
40
30
20
10
0
-0.6
-0.4
-0.2
0.0
0.2
0.4
0.6
0.8
1.0
Thermal axial strain (%)
1st Cycle
2nd Cycle
3rd Cycle
4th Cycle

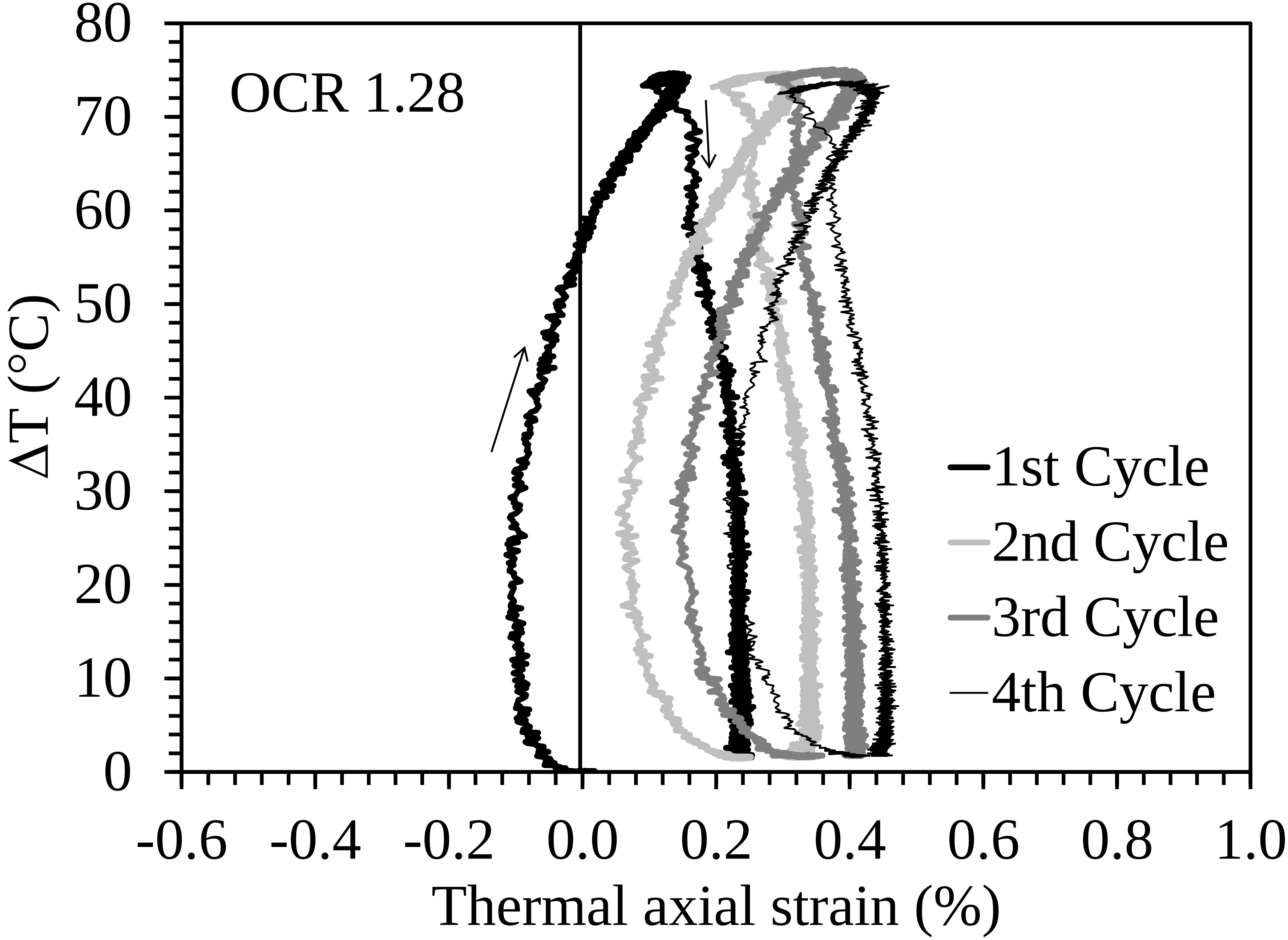

OCR 1.28
ΔT (°C)
80
70
60
50
40
30
20
10
0
-0.6
-0.4
-0.2
0.0
0.2
0.4
0.6
0.8
1.0
Thermal axial strain (%)
1st Cycle
2nd Cycle
3rd Cycle
4th Cycle

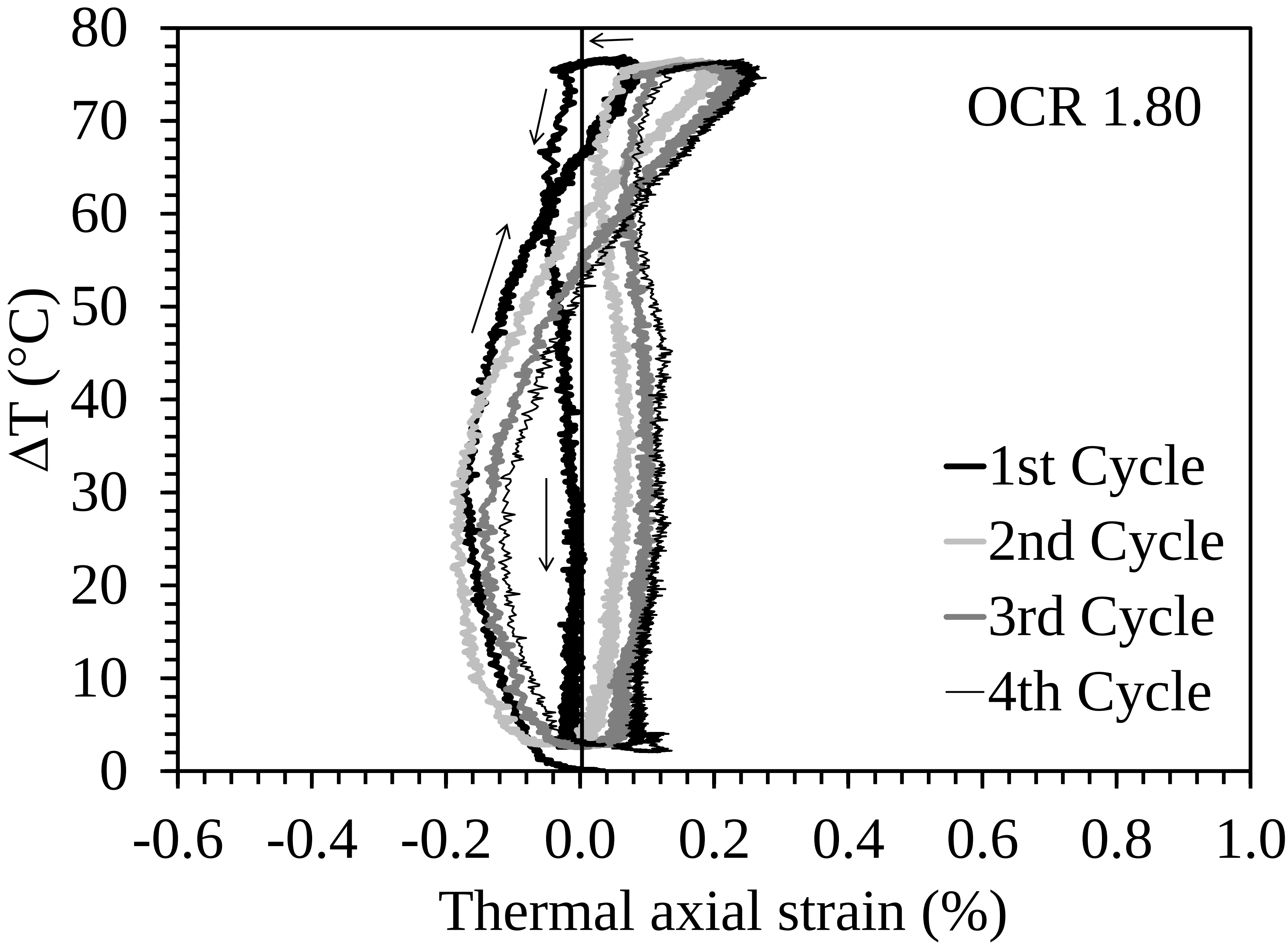

80
70
60
50
40
30
20
10
0
ΔT (°C)
-0.6
-0.4
-0.2
0.0
0.2
0.4
0.6
0.8
1.0
Thermal axial strain (%)
OCR 1.80
1st Cycle
2nd Cycle
3rd Cycle
4th Cycle

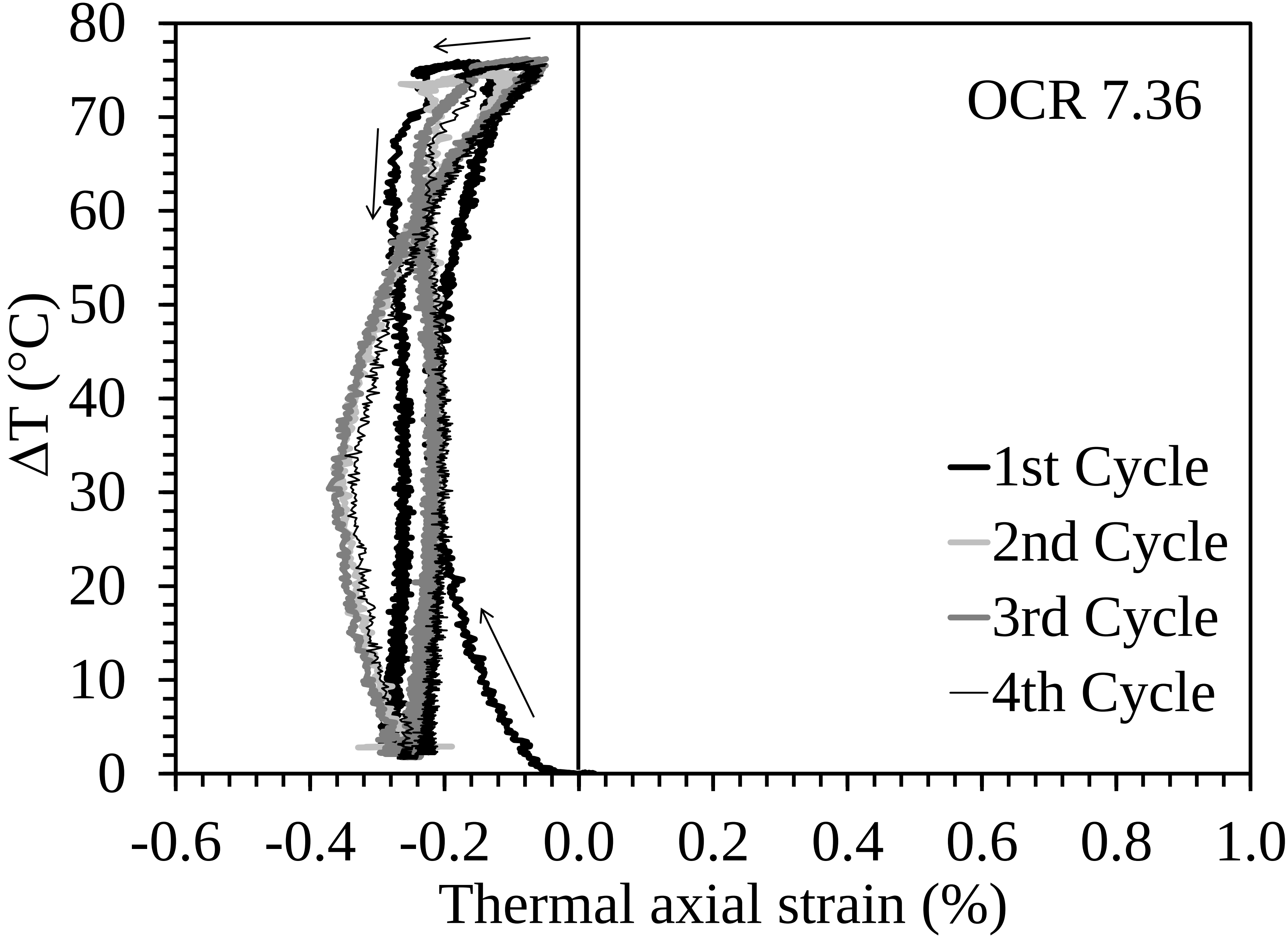

OCR 7.36
1st Cycle
2nd Cycle
3rd Cycle
4th Cycle
ΔT (°C)
Thermal axial strain (%)
0
10
20
30
40
50
60
70
80
-0.6
-0.4
-0.2
0.0
0.2
0.4
0.6
0.8
1.0

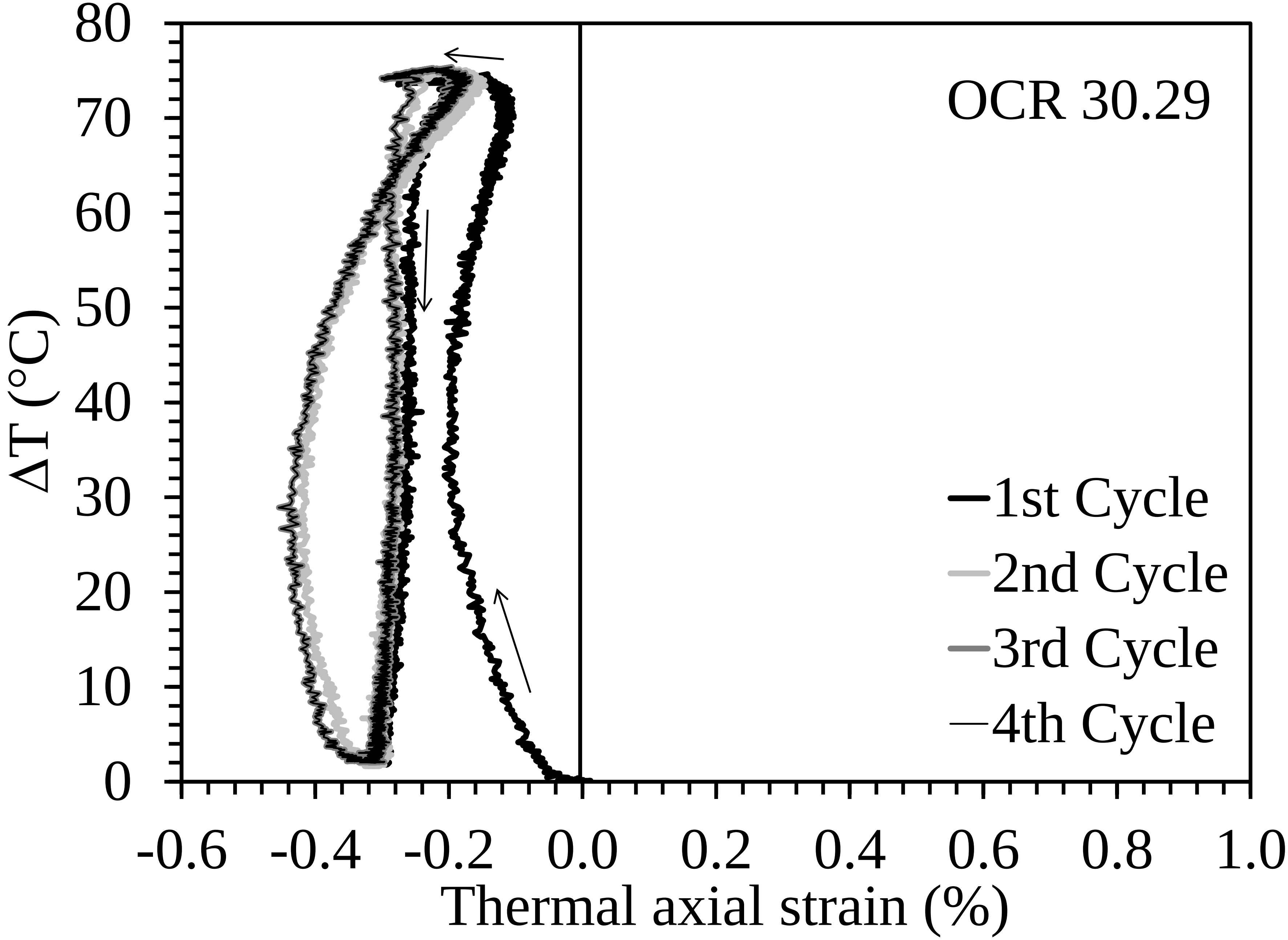

80
70
60
50
40
30
20
10
0
ΔT (°C)
-0.6
-0.4
-0.2
0.0
0.2
0.4
0.6
0.8
1.0
Thermal axial strain (%)
OCR 30.29
1st Cycle
2nd Cycle
3rd Cycle
4th Cycle

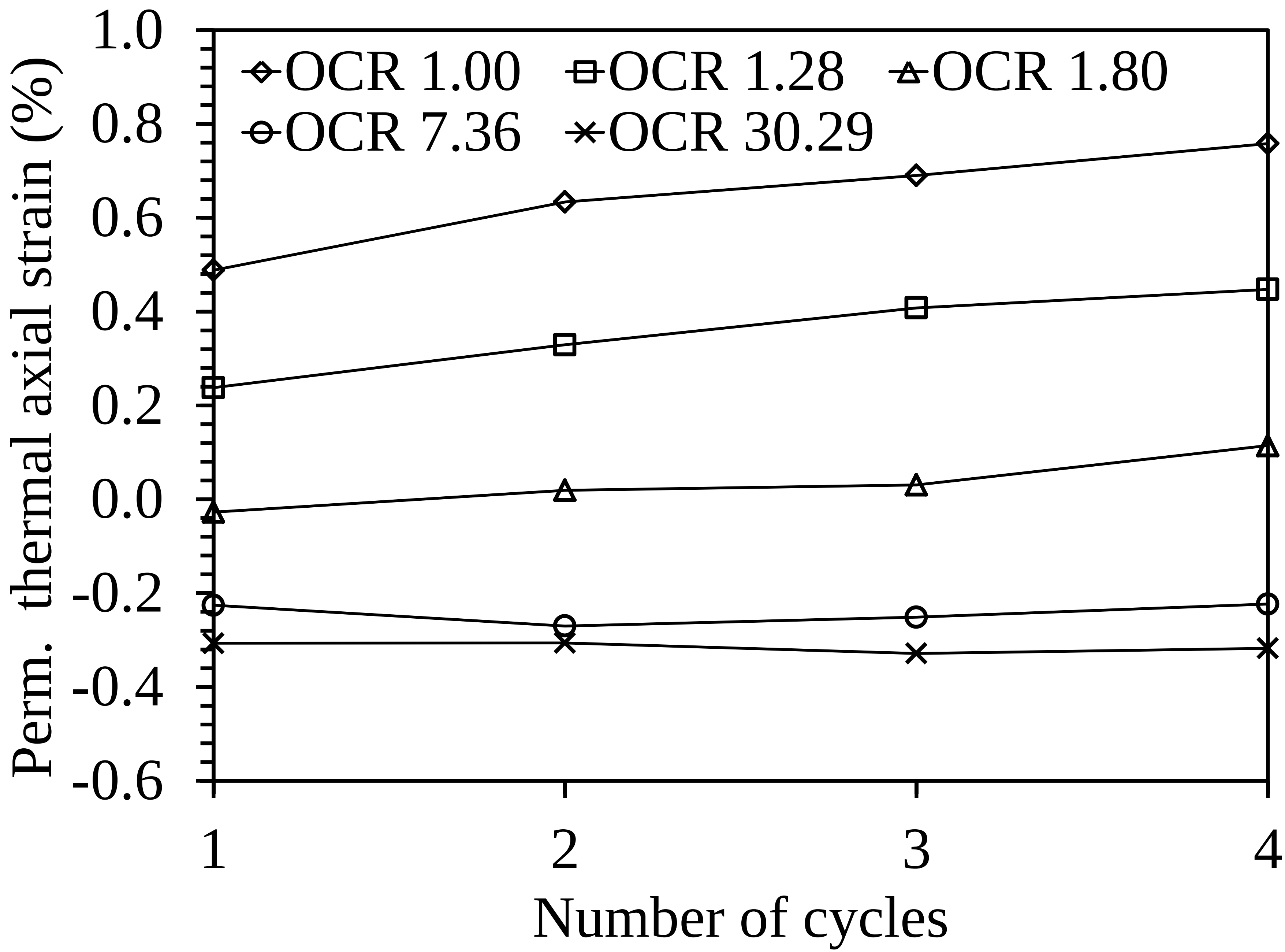

OCR 1.00
OCR 1.28
OCR 1.80
OCR 7.36
OCR 30.29
1.0
0.8
0.6
0.4
0.2
0.0
-0.2
-0.4
-0.6
Perm. thermal axial strain (%)
1
2
3
4
Number of cycles

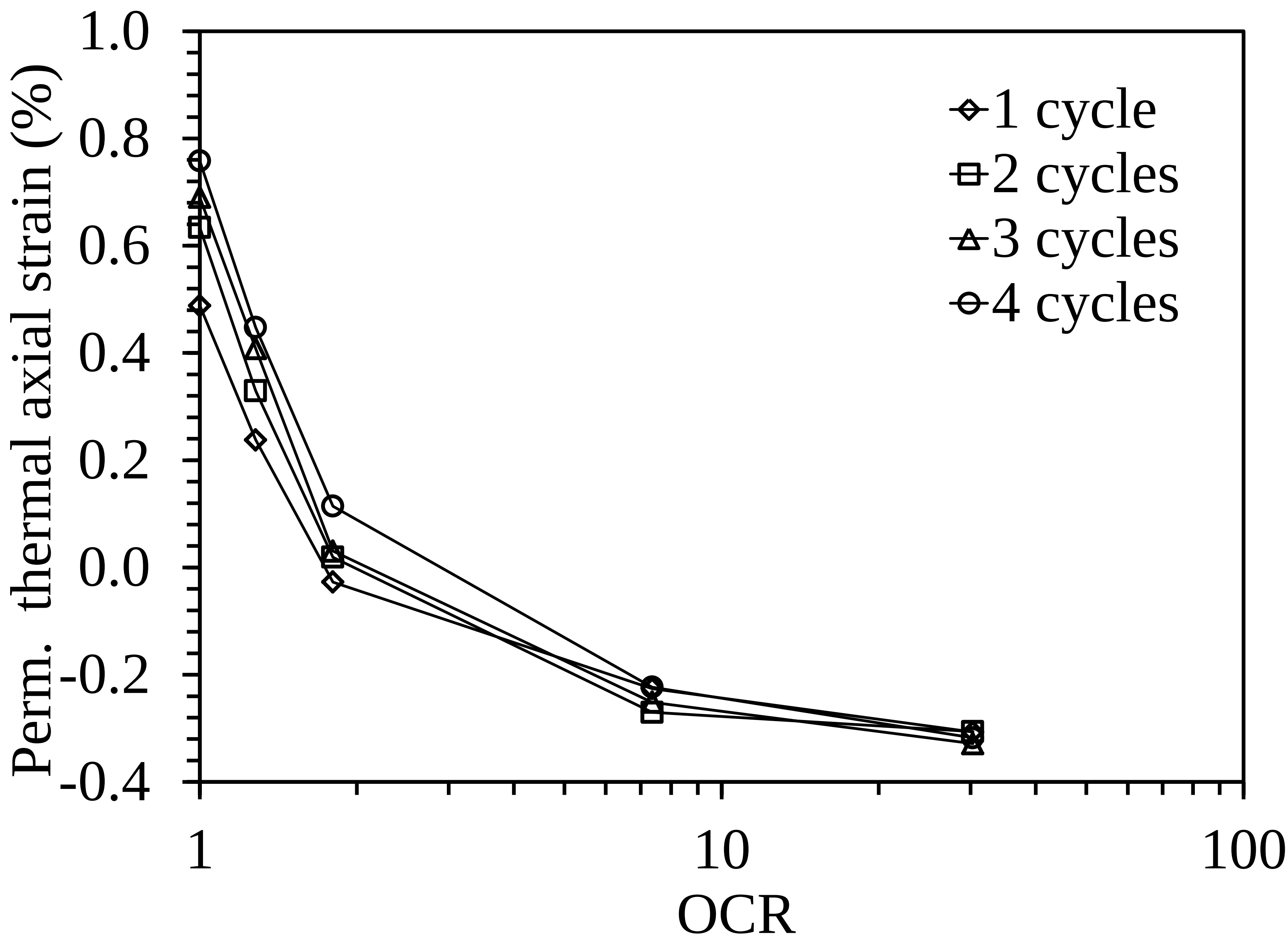

1.0
0.8
0.6
0.4
0.2
0.0
-0.2
-0.4
Perm. thermal axial strain (%)
1
10
100
OCR
1 cycle
2 cycles
3 cycles
4 cycles

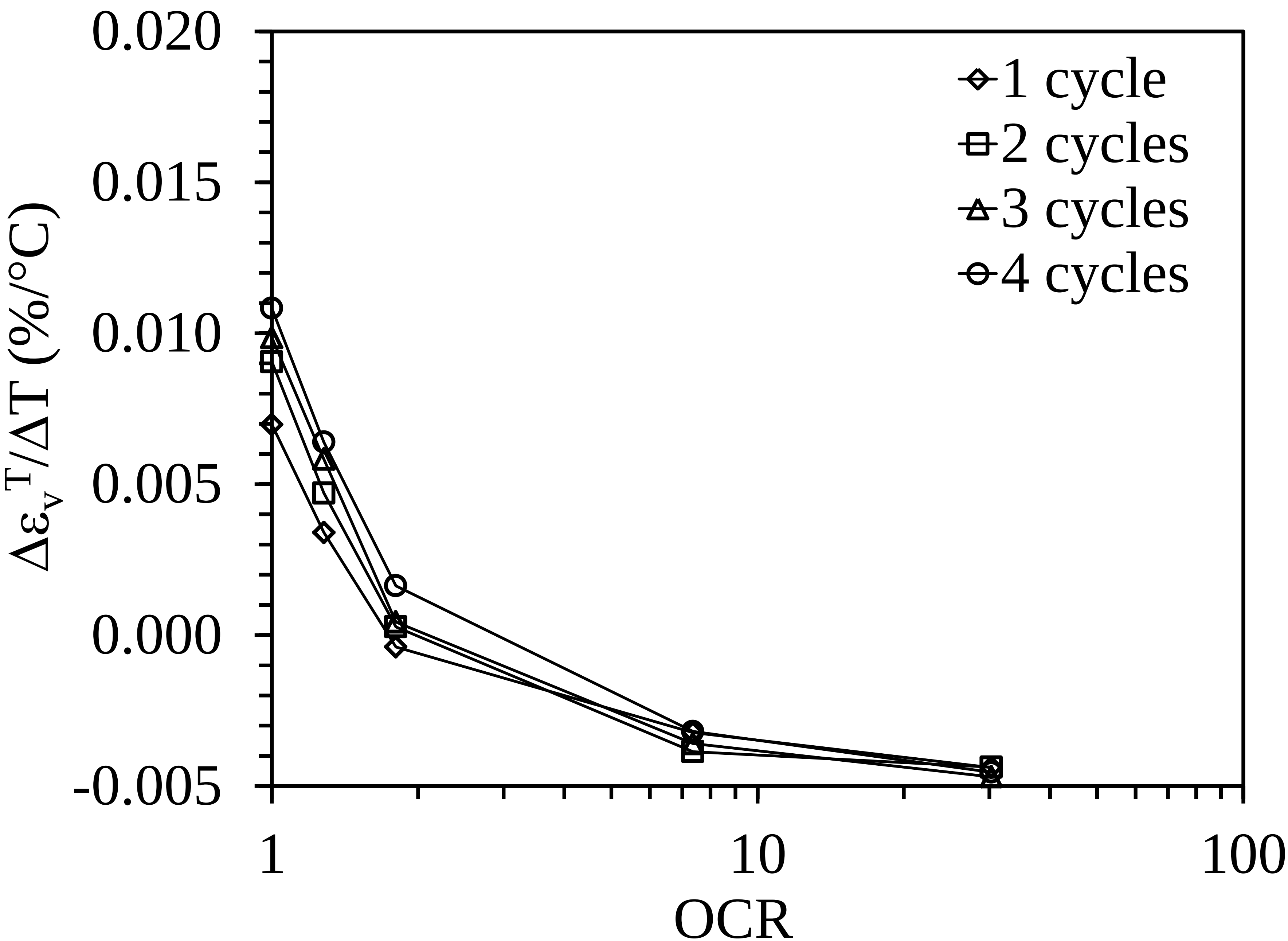

0.020
0.015
0.010
0.005
0.000
-0.005
1
10
100
OCR
Δε_v^T/ΔT (%/°C)
1 cycle
2 cycles
3 cycles
4 cycles